REVIEW

Check for updates

Nanostructured silicate catalysts for environmentally benign Strecker-type reactions: *status quo* and *quo vadis*†

Vladimir V. Kouznetsov [ID] *[a] and José G. Hernández [ID] [b]

Chemical processes are usually catalytic transformations. The use of catalytic reagents can reduce the reaction temperature, decrease reagent-based waste, and enhance the selectivity of a reaction potentially avoiding unwanted side reactions leading to green technology. Chemical processes are also frequently based on multicomponent reactions (MCRs) that possess evident improvements over multistep processes. Both MCRs and catalysis tools are the most valuable principles of green chemistry. Among diverse MCRs, the three-component Strecker reaction (S-3-CR) is a particular transformation conducive to the formation of valuable bifunctional building blocks (α-amino nitriles) in organic synthesis, medicinal chemistry, drug research, and organic materials science. To be a practical synthetic tool, the S-3-CR must be achieved using alternative energy input systems, safe reaction media, and effective catalysts. These latter reagents are now deeply associated with nanoscience and nanocatalysis. Continuously developed, nanostructured silicate catalysts symbolize green pathways in our quest to attain sustainability. Studying and developing nanocatalyzed S-3-CR condensations as an important model will be suitable for achieving the current green mission. This critical review aims to highlight the advances in the development of nanostructured catalysts for technologically important Strecker-type reactions and to analyze this progress from the viewpoint of green and sustainable chemistry.

Introduction

Multicomponent reactions (MCRs) can be defined as processes in which three or more reactants are introduced concomitantly, and the final product contains significant parts of these starting materials. Based on MCRs, chemical processes in the preparation of diverse highly complex, functionalized molecules, such as fine chemicals, pharmaceuticals, agrochemicals or advanced materials, are a topic of significant interest in academia and industry.[1–4] Possessing many apparent advantages over multistep processes, such as high efficiency, atom economy, reduced waste generation, and time and energy economy, almost all MCRs comply with the majority of Anastas and Warner's principles of green chemistry, making the use of MCRs an ideal synthetic strategy.[5] However, to be a practical synthetic tool, MCRs need to be completed with alternative energy input systems, safe reaction media, and effective catalysts. These

latter reagents are now strongly linked to nanoscience and nanocatalysis.[6,7] In 2003, Bell pointed out that most industrial catalysts consist of nanometer-sized particles dispersed on high-surface-area supports, and thus, catalyst performance can be sensitive to particle size[8] because the surface structure and electronic properties can change greatly in this size range.[9] Nanocatalysts, *i.e.*, nanomaterials, possess special properties and functions with at least one external dimension that measures 100 nanometers (1 nm = 10^{-9} m) and include nanoobjects such as nanoparticles, nanofibers (rods, tubes), and nanoplates. Indeed, catalysts are used in 90% of processes in the chemical industry, and thus, (nano)-catalysts and the multitude of products prepared through their use are fundamental to modern life.[10] Constantly developed nanocatalysts represent green pathways in our pursuit toward attaining sustainability[11] because the nanomolecular sizes of catalysts (particularly metal catalysts[12]) offer a desirable increase in the surface area for the improvement of reactions along with a change in properties to help adopt environmentally friendly reaction procedures.[13]

One of the oldest known MCRs is the Strecker reaction, which basically allows α-amino nitriles to be obtained. These α-amino nitriles are usually prepared from available aldehydes (or ketones), amines, and a cyanide anion source and can be transformed into biologically important α-amino acids and other related valuable products or/and intermediates, such as α-

[a]Laboratorio de Química Orgánica y Biomolecular, CMN, Universidad Industrial de Santander, Parque Tecnológico Guatiguará, Km 2 Vía Refugio, Piedecuesta 681011, Colombia. E-mail: kouznet@uis.edu.co; vkuznechnik@gmail.com; Tel: +57 7 634 4000 ext. 3593

[b]Grupo Ciencia de los Materiales, Instituto de Química, Facultad de Ciencias Exactas y Naturales, Universidad de Antioquia, Calle 70 No. 52-21, Medellín, Colombia. E-mail: joseg.hernandez@udea.edu.co

† Dedicated to the memory of Adolph Strecker (1822–1871) on the 200th anniversary of his birth.

amino aldehydes (ketones), α-amino alcohols, 1,2-diamines, and heterocycles (Scheme 1).[14]

So-called Strecker intermediates, α-amino nitriles are not only fascinating, versatile, and valuable bifunctional building blocks in organic synthesis but are also one of the most important prebiotic precursors in the synthesis of nucleic acids, peptides, and proteins, which are essential biomacromolecules to all life on Earth.[15–18] Initial α-amino nitrile formation from aldehydes, ammonia, and hydrogen cyanide or natural cyanide transferring agents could be realized under the conditions of a prebiotic atmosphere in hydrothermal (aqueous) or dry (nonaqueous) environments in the presence of some mineral-organic systems, such as clays (e.g., phyllosilicates such as kaolinite and smectite or montmorillonite) or metal oxide-based minerals (ZnO, TiO$_2$, NiO, Fe$_2$O$_3$, among others)[19] and metal sulfide-based mineral depositions, such as pyrite (FeS$_2$) or chalcopyrite (CuFeS$_2$).[20]

When these natural minerals are dispersed into a polymer medium, they can transform into independent units at the nanometer scale, hence the name "nanocomposite materials", and these prebiotic mineral systems can act as nanostructured catalysts that facilitate α-amino nitrile formation. Thus, there is an agreement that the interaction of organic molecules with the surfaces of naturally occurring minerals, especially clays, iron sulfides, titanium dioxide, and silica/silicates, might have provided catalytic sites that could have contributed to prebiotic small organic molecule formation.[21,22]

Therefore, current studies on the reactivity of nano-structured catalysts with their high surface area in Strecker-type reactions take on triple relevance for the following key aspects: (i) development of nanoscience and nanomaterial-based catalysts as significant and attractive heterogeneous catalysts; (ii) improvement and understanding MCR processes in general and Strecker-type reactions in particular, and (iii) comprehension of how life on Earth might have originated. Additionally,

understanding how nanocatalysis for Strecker-type reactions operates would certainly complement our comprehension of homogeneous and heterogeneous catalysis for this trans-formation, thus strengthening the field of catalysis research as a whole. Importantly, due to their state of matter, nanomaterial-based catalysts can be considered as species that exhibit both homogeneous and heterogeneous nature, therefore profiting from the corresponding advantages of their counterparts (e.g., (i) simple catalyst separation and recovery as for heterogeneous catalysts with (ii) high contact between the reagents and the catalyst often matching the high catalytic activity found in homogeneous catalytic systems). Thus, this revision of recent scientific literature aims to highlight the advances in the development of nanostructured silicate catalysts for techno-logically important Strecker-type reactions and to analyze this progress from the viewpoint of green and sustainable chem-istry, discussing the advantages and disadvantages of existing protocols based on the use of nanocatalytic systems for α-amino nitrile formation. To achieve these goals, this review article includes the following sections: nanocatalysis and traditional catalytic systems, mesoporous molecular sieves (MCM-41 materials, SBA-15 derivatives, and clays), mesoporous molec-ular sieve-supported metal complexes, Fe$_3$O$_4$@SiO$_2$ core–shell nanoparticles and asymmetric S-3-CR condensations under nanocatalysis, in which the advantages and drawbacks of each presented nanocatalyst, their synthesis and application are critically discussed.

Nanocatalysis and traditional catalytic systems

Catalytic events occur at several scales of length, shape, and time. Generally, traditional catalysts consist of active metal phases and less active or inactive solid carriers to expand the whole accessible working area and material utilization. These
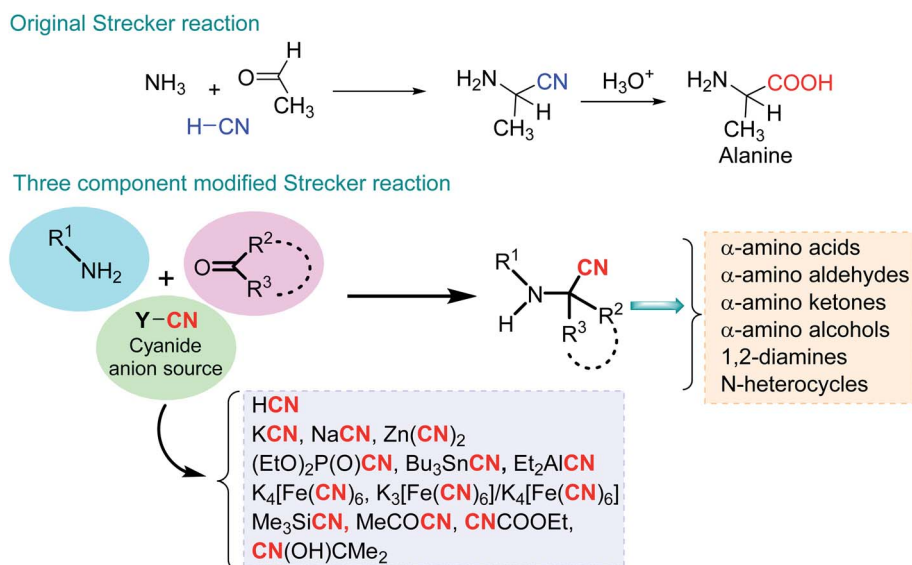
Scheme 1 The Strecker reaction and its modified reaction are three-component condensation reactions.

catalysts typically work within the different dimensional regimes of several to a few tens of nanometers. Their processing often requires several steps, mainly impregnation, precipitation, coating, rewashing, ion exchange, pulverization, drying, heat treatment, reduction, and activation, through which the metal clusters or active nanoparticles can be dispersed on the carriers; thus, these catalyst systems basically depend on the precise mechanistic details of all the abovementioned processes.[23]

Subsequently, the structure and composition of catalysts may change during reactions, especially under high temperature and pressure conditions, which can hinder understanding the interaction between the catalyst and the supporting solid that in turn precludes the effective use of catalytic systems. In the nanocatalysis area, the limited size and roughness of the surface of suitably prepared nanoparticles affect their catalytic function, providing them with fine-tuned local electronic properties that have a direct influence on the reaction rate. Catalytic materials can now be prepared with better accuracy *via* nanotechnology-enabled processes controlling crystal structure, morphology, and surface composition; thus, the selectivity and reactivity of the nanocatalysts have vital importance.[6,23]

Current nanostructured catalysts comprise multicomponent active nanometal phases with highly porous nanomaterial supports, which successfully improve the structure or properties of active materials. Diverse and numerous nanocatalysts can be classified into three general groups, *e.g.*, metal-based, carbon-based, and quantum dot catalysts. On numerous occasions, micro- and mesoporous silica play a crucial role as a matrix, facilitating control over the arrangement of the nanocatalysts. Sometimes, nanostructured catalysts are based on a magnetic matrix, and these so-called magnetic nanosystems of various chemical natures and morphologies have become popular.[24] These types of nanocatalysts are expected to display the benefits of both homogenous and heterogeneous catalysts, specifically, high efficiency and selectivity, stability, and easy recovery/recycling acting as a bridge between homogenous and heterogeneous catalysts.[11,25,26] Recyclability along with heterogeneous catalysts could drastically eliminate harsh work-ups and therefore could minimize the use of unnecessary substances (*e.g.*, VOC compounds), energy, and time needed. These factors can directly affect the cost of chemical processes.

In the last decade, these catalysts have been suggested and used to successfully model the three-component Strecker reaction (S-3-CR) of aldehydes (ketones) **1**, amines **2**, and trimethylsilyl cyanide **3** (Me$_3$SiCN, TMSCN) as an available and potent cyanation agent to provide diverse α-amino nitriles **5** (Scheme 2). Usually, the classical Strecker reaction is carried out in an aqueous solution, and the work-up procedure is tedious. Thus, varied reaction conditions and an endless number of catalysts have been employed in this classical three-component reaction.[14]

According to the literature, most investigations on the S-3-CR methodology refer to the synthesis of 2-aryl-2-(arylamino) acetonitriles **5a**, obtained from arylamines and aromatic aldehydes (type-I) or 2-aryl-2-(heterocyclan-1-yl)acetonitriles **5b**, prepared from the same aldehydes and cyclic secondary amines

(*e.g.*, NH-pyrrolines and NH-piperidines) (type-II). Both acetonitrile skeletons are formally tertiary α-amino nitrile derivatives. Other acetonitrile skeletons with quaternary nitrile groups derived from arylamines and aralkyl ketones (**5c**, type-III) or cyclic ketones (**5d**, type-IV) are still restricted because ketones show lower reactivity in comparison with aldehydes due to more steric hindrance around the carbonyl group of ketones. Consequently, the initial sections focus on the preparation of α-amino nitriles types I and II. In the next sections, it will be seen that the increase in molecular complexity of a silica-based nanocatalyst allows the preparation of α-amino nitrile types III and IV more easily. These synthetic details will be considered, pointing out the advantages and shortcomings of nanostructured catalysts.

Mesoporous molecular sieves

MCM-41 and its derivatives

Perhaps one of the simplest and most studied catalysts based on silicate materials in the field of catalysis and organic synthesis is mesoporous molecular sieves,[27] which have high surface areas, large pore volumes, and a well-defined pore structure with a pore diameter between 2 and 50 nm. Their successful application as catalysts and catalyst supports dates to 1992, when the preparation and characterization of mesoporous silica material, the so-called famous MCM-41 (Mobil catalytic material number 41), were reported by Beck *et al.*[28] Researchers from the Mobil Oil Company prepared this ordered mesoporous silica and aluminosilicate material with a hexagonal arrangement of uniform mesopores whose cylindrical pore size can be adjusted from 1.5 to larger than 10 nm (Fig. 1A). Thirty years have passed, and fascinating interest in MCM-41 applications has not diminished despite its low intrinsic acidity strength. However, its great porosity and uniform structure offer a very attractive and convenient technique for the immobilization of different catalysts. This material's flexibility in functionalization with a broad variety of organic groups (more particularly with organosiloxane agents) of mesoporous silica materials is fantastic. Possessing a large number of silanol groups on internal surfaces, Si-based MCM-41 can be easily functionalized by incorporating heteroatoms and metal ions, such as Al, Fe, Ti, V, Mn, and Zr, or by covalent grafting with various organic or inorganic moieties. Such modifications can be accompanied by the formation of both Brønsted and/or Lewis acid sites without a substantial change in the hexagonal structure.

Functionalized MCM-41 analogs containing metal ions have been applied in the field of synthetic organic chemistry in recent years. In particular, nanoordered Al-MCM-41, Fe-MCM-41, Zr-MCM-41, and B-MCM-41 materials (Fig. 1B) have been tested as heterogeneous catalysts in Strecker-type reactions.

Another way to enhance surface acidity is by anchoring inorganic or organic acids through the covalent postgrafting methodology. In general, functionalizing of MCM-41 with –SO$_3$H groups is usually performed through direct synthesis (cocondensation reactions of siloxane and organosiloxane precursors in the presence of the corresponding structure-
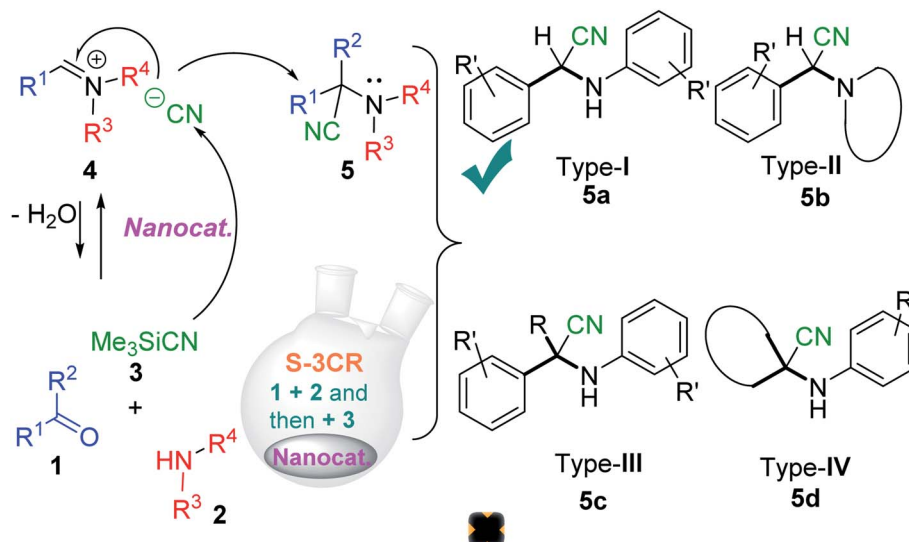
Scheme 2 S-3-CR condensations of aldehydes (ketones), amines, and TMSCN provide diverse α-amino nitriles.

directing agent) or a postgrafting process, which is based on the modification of the silica surface with organic groups through silylation reactions. Diverse acid-anchored MCM-41 nanomaterials, *i.e.*, sulfonic acid (MCM-41-SO₃H), tungstic acid (MCM-41-WO₃H), 3-(trimethoxysilyl)propane-1-sulfonic acid (MCM-41-PSA), and others (Fig. 1C) have been continuously
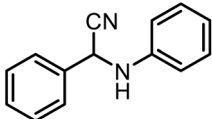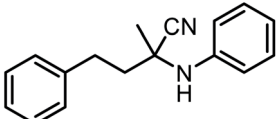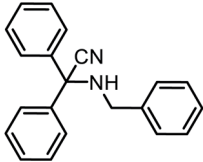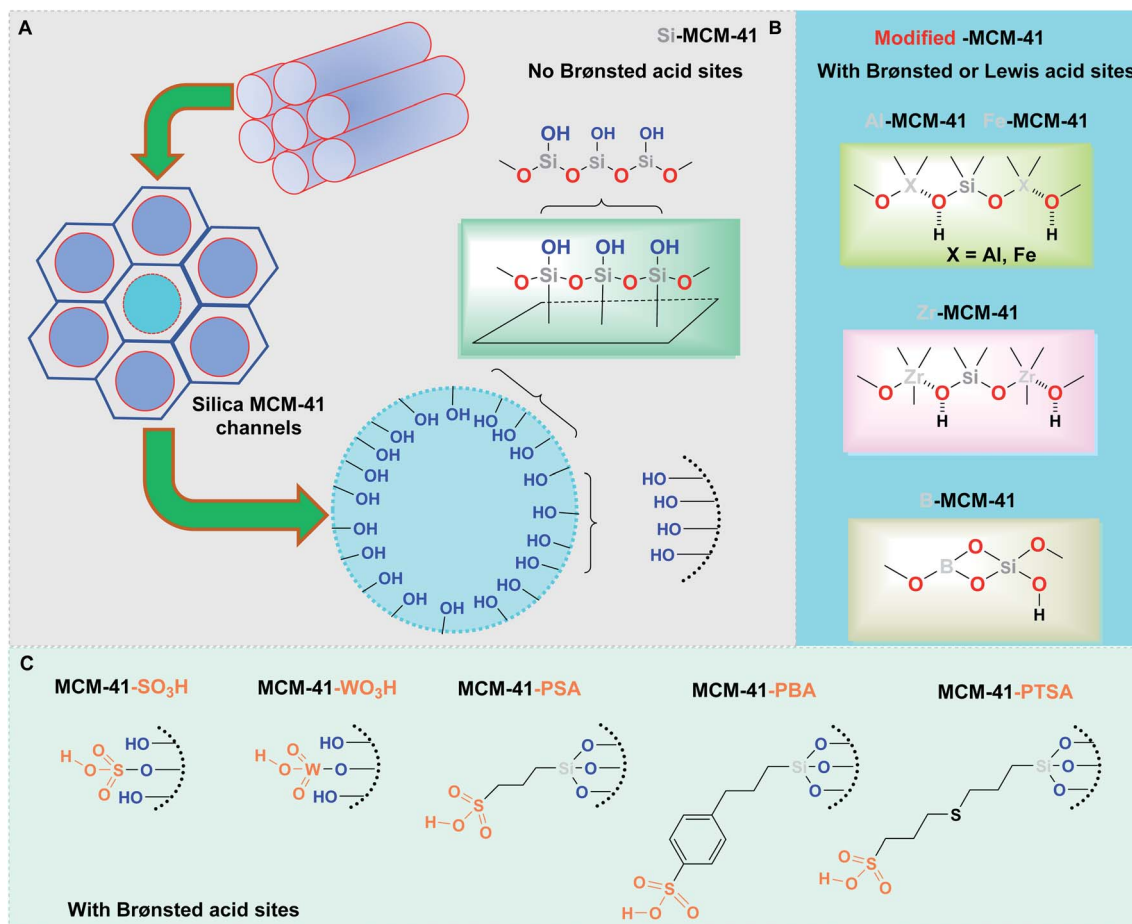

Fig. 1 General structural representation of mesoporous MCM-41 and its modified analogs used in the S-3CR processes.

Table 1 Selected examples: α-amino nitrile formation using pure MCM-41 and aluminum-incorporated MCM-41 as nanocatalysts

Nanocatalyst	6, Type-I	7, Type-III	8, Type-III
Si-MCM-41	95%, 5 min (solvent-free, rt)	61%, 24 h (CH_2Cl_2, rt)	Not tested
Al-MCM-41	Not tested	97%, 24 h (CH_2Cl_2, rt)	Not obtained

developed and proposed as catalysts for some concrete chemical transformations. Exhibiting potential advantages over homogeneous systems (simplified recovery and reusability, the potential for incorporation into continuous reactors and microreactors) of these materials could lead to novel environmentally benign chemical procedures for academia and industry. It is noteworthy that even though catalyst-free S-3-CR reactions with TMSCN have been described,[29,30] in recent years, a large spectrum of innumerable categories of homogeneous and heterogeneous Lewis or Brønsted acids, bases, metal complexes, and organic reagents or catalysts have been proposed to promote this historical and important MCR.[14] Furthermore, many of these catalysts are deactivated or sometimes decomposed by amines and water that exist during imine formation. As a result, a "clean and green" procedure for α-amino nitriles 5 based on cost-effective, nontoxic, and recyclable catalysts is still far from practical. In a general context, efforts to find alternative and environmentally benign synthetic routes are one of the most important objectives in the protection of the ecosystem and are vital for the development of life and life processes. In particular, research and development of solid-activated silica-based mesoporous catalysts and their application in vital MCRs, such as Strecker-type reactions, can minimize waste and avoid pollution during chemical processes.

Despite weak acidity, pure MCM-41 catalyzes well three-component reactions of benzaldehydes or methyl ketones (benzylacetones), amines, and TMSCN, giving corresponding tertiary and quaternary α-amino nitriles, such as 6–7 (Table 1).

Their efficient preparation was carried out under solvent-free conditions[31] or organic solvent medium (CH_2Cl_2)[32] at room temperature. The S-3-CR using the Si-MCM-41 catalyst under solvent-free conditions allowed 6 to be obtained in high yields (95%) in a very short reaction time (5 min) at room temperature.[31] When the Si-MCM-41 catalyst that provided α-amino nitrile 7 in dichloromethane at a 61% yield was replaced by Al-MCM-41 with a Si/Al ratio of 20, the desired product was obtained at a 97% yield after 24 h of reaction time.[32] However, the desired quaternary α-amino nitrile 8 was not obtained under the same reaction conditions. It should be noted that

amorphous silica-alumina, SiO_2–Al_2O_3, gave the desired product 7 at lower yields (40%).[32]
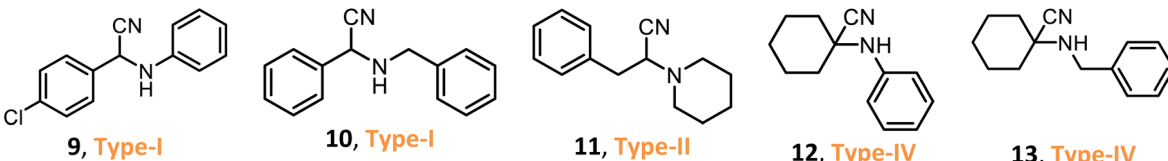
Si-MCM-41 was prepared following the procedure given by Ryoo and Kim[33] with some modifications using a mixture of tetraethylorthosilicate (TEOS) as a silica source and cetyltrimethylammonium bromide (CTAB) as a structure-directing agent in the presence of diethylamine and deionized water at pH 8.5 (1 M HCl) to obtain a solid product that was filtered and dried at 45 °C for 12 h and then calcined at 550 °C for 5 h. Al-MCM-41 was obtained by a direct hydrothermal method according to the original procedure[34] with some modifications using CTAB as a template with a gel composition of $CTAB : SiO_2 : NaAlO_4 : NaOH : NH_3 : H_2O$ whose molar ratio was 1.1 : 20 : 1.0 : 5.5 : 1.1 : 940. This gel mixture was initially stirred for 1 h at room temperature and heated to 97 °C. Its common treatment (heating, pH adjustment, drying, and calcination) allowed the preparation of the desired nanomaterial, whose surface area and pore volume were 993 m^2 g^{-1} and 1.08 cm^3 g^{-1}, respectively.[35]

It is interesting to note that the amorphous SiO_2–Al_2O_3 catalyst has a smaller surface area (157 m^2 g^{-1}) than the aluminum-incorporated MCM-41 catalyst, and it would be concluded that the high yield produced by Al-MCM-41 is principally due to its high surface area. Similar to the Al-MCM-41 catalyst, mesoporous crystalline iron-, zirconia- and boron-containing MCM-41 molecular sieves can also be prepared by direct hydrothermal synthesis. The precursor solution for the first two materials consists of CTAB, water, TEOS, 1 N hydrochloric acid, and the respective Fe (Zr)-containing salts, *i.e.*, ferric chloride, ferric oxalate, ferric nitrate, and zirconium(IV) chloride or zirconyl chloride octahydrate.[36–40] To prepare nano-ordered B-MCM-41 with active boron sites (Si/B ratio of 20), initial gels with the following molar composition were used: SiO_2:$0.05B_2O_3$:$0.10CTAB$:$0.33NaOH$:$70H_2O$. The integration of boron into the pore wall was made in the form of boric acid (H_3BO_3) in the presence of NaOH.[41,42]

Despite the limited information on the catalytic activity of these modified molecular sieves as nanocatalysts in S-3-CR condensation, an attempt to compare them has been made. Table 2 includes the results of the synthesis of selected α-amino

Table 2 Comparative analysis of the catalytic role of modified MCM-41 nanomaterials with the active Al, Fe, Zr, and B sites in S-3-CR procedures

| Nanocatalyst	9, Type-I	10, Type-I	11, Type-II	12, Type-IV	13, Type-IV
Si-MCM-41	95%, 5 min (solvent-free, rt)	90%, 30 min (solvent-free, rt)	Not tested	Not tested	Not tested
Al-MCM-41	Not tested	100%, 0.5 h (CH_2Cl_2, rt)	100%, 3 h (CH_2Cl_2, rt)	Not tested	91%, 3 h (CH_2Cl_2, rt)
Fe-MCM-41	95%, 6 h (CH_2Cl_2, rt)	Not tested	Not tested	Not tested	Not tested
Zr-MCM-41	Not tested	84%, 25 min (CH_3CN, reflux)	Not tested	Not tested	Not tested
B-MCM-41	98%,1.5 h (EtOH, rt)	91%, 2.25 h (EtOH, rt)	Not tested	89%, 6.75 h (EtOH, rt)	Not tested

nitriles **9–13** of different skeleton types. It is not difficult to observe the lack of data to compare the catalytic efficiency. However, preliminary conclusions can be drawn. The solvent-free S-3-CR method using pure MCM-41 results in a more rapid procedure for the preparation of α-amino nitrile type I, but hot EtOH must be used to separate the catalyst and the crude products by subsequent filtration, and this is not as efficient as it seems.[31] The Al-MCM-41 nanomaterial appears to be a more versatile catalyst working well in the generation of diverse kinds of α-amino nitriles, types I–IV;[32] however, dichloromethane is toxic, an inhalation hazard, a skin irritant, and may cause cancer of the pancreas, liver, and lungs. Thus, this chlorinated solvent with a low boiling point must be substituted in the manufacturing processes of active pharmaceutical ingredients, such as α-amino nitriles. Compared to Si-MCM-41, the densities of both Lewis and Brønsted acid sites and the strength of the acidity on the Zr-MCM-41 were significantly increased, suggesting that the incorporation of zirconium greatly enhances the acidity of the material with the possible strong polarization of the $Si–O^{-\delta}\cdots Zr^{+\delta}$ linkages.[43] It should be noted that the specific surface area and pore volume of the Zr-MCM-41 sample used in the S-3CR were 676.2 $m^2\ g^{-1}$ and 1.2854 $cm^3\ g^{-1}$, respectively, which are comparable to those of Al-MCM-41.[40] Therefore, it is strange that this acid nanocatalyst has not been tested in a more diverse series of α-amino nitriles; moreover, Zr-MCM-41-catalyzed S-3-CRs were realized in refluxing MeCN, and the reaction conditions were more drastic than those of other S-3-CRs, and the reactions were performed at room temperature. Similar to Zr-MCM-41, the Fe-MCM-41 nanocatalyst was not thoroughly tested or studied in S-3-CR, but it seems that its catalytic potency is close to that of Al-MCM-41. Finally, possessing a low acidity comparable to that of Si-MCM-41, B-MCM-41 shows good potency as a catalyst, outperforming the Fe-MCM-41 and Si-MCM-41 nanomaterials in catalytic activity for the rapid formation of different types of α-

amino nitriles.[42] It appears that in the case of heteroatom-incorporated MCM-41 molecular sieves, the high acidity of nanomaterials and increasing reaction temperature are counterproductive to the formation of Strecker products. The most important advantages of these methodologies are low catalyst loading, excellent yields, a very simple work-up procedure (separation through filtration of catalysts), easy catalyst handling, and catalyst recyclability. Comparing the results and considering current green trends in organic chemistry, among the heteroatom-incorporated MCM-41 molecular sieves, the B-MCM-41 nanomaterial can be chosen as one of the most promising nanocatalysts for Strecker-type reactions.

Some experimental data on these transformations, *i.e.*, catalytic cycles of the S-3-CR demonstrated that formation of an imine intermediate is the key step in the one-pot three-component Strecker reaction catalyzed by the pure MCM-41 and its modified analogs[14,31] (Scheme 3A). The characterization of these nanocatalysts was usually performed by electron microscopes using transmission electron microscopy (TEM) and scanning electron microscopy (SEM) techniques (Scheme 3B).

To date, numerous recoverable and heterogeneous nonmetal-incorporated catalysts have been designed and used. Among these, the use of nanosilica (crystalline SiO_2) in chemistry and synthetic methodology is very attractive, possessing a particle size of −15 to 20 nm and a specific surface area of 559–685 $m^2\ g^{-1}$. This low-cost, physiologically inert, and porous material is fabricated from sodium silicate and ethyl orthosilicate as raw materials. However, pure SiO_2 is not active in the S-3-CR, as indicated by Iwanami *et al.*,[32] while silica sulfuric acid (SSA, SiO_2–SO_3H) is very effective, as demonstrated by Chen and Lu.[46] This reusable green and inexpensive heterogeneous acid catalyst has been widely investigated[47–51] since 2001, when Zolfigol described its preparation by using a simple reaction of neat chlorosulfonic acid and silica gel (Fig. 2A).[52] The operational
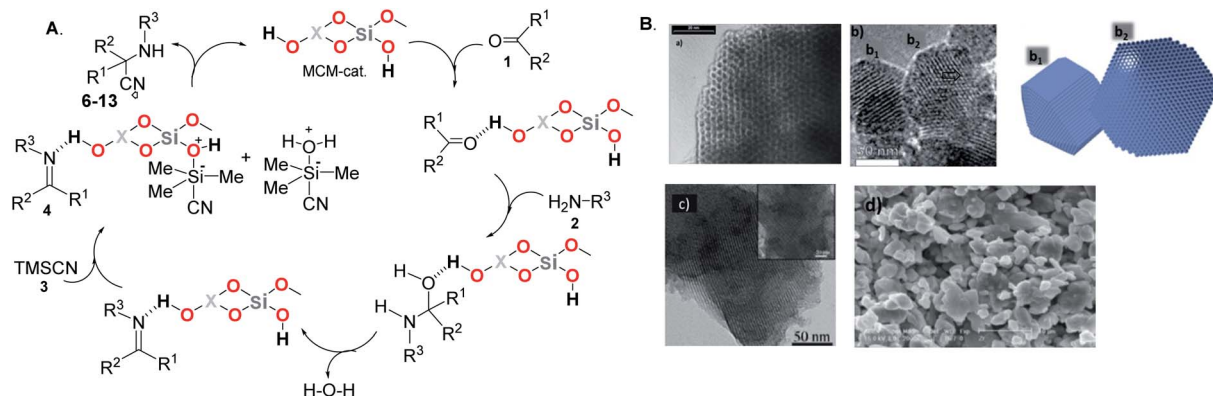
Scheme 3 (A) Plausible mechanism for the Strecker reaction of carbonyl compounds and amines with TMSCN catalyzed by pure MCM-41 and its metal-incorporated analogs where X = Si, Al, Fe, Zr, and B heteroatoms. (B) Images of the surface of the used MCM-41-based catalysts: (a) TEM image of Si-MCM-41 silica. Reproduced from ref. 44 with permission from Elsevier, copyright [2016]; (b) TEM micrograph of Al-MCM-41 nanoparticles showing the channels and schematic depiction of the two particles marked (b₁) and (b₂) in the figure shown at left. Reproduced from ref. 45 with permission from the Royal Society of Chemistry, copyright [2014]; (c) TEM image of Fe-MCM-41 calcined at 550 °C. Reproduced from ref. 38 with permission from Elsevier, copyright [2006]; (d) SEM micrograph of the freshly activated Zr-MCM-41. Reproduced from ref. 40 with permission from Elsevier, copyright [2011].

simplicity and recyclability of SSA can be exploited in industry for the synthesis of various drugs, pharmaceuticals, or agrochemicals.

Chen and Lu[46] and others reported a practical method for the synthesis of diverse α-amino nitriles through a one-pot three-component coupling of aldehydes (but not ketones), amines, and TMSCN catalyzed by SSA at room temperature in toxic, nongreen solvents (dichloromethane or acetonitrile).[53,54] These SSA-catalyzed Strecker reactions allow interesting girgensohnine alkaloid-like α-amino nitriles **5b** (type II) to be obtained; among them, 2-aryl-2-(piperidin-1-yl)- and 2-aryl-2-(pyrrolidin-1-yl)acetonitriles **14** and **15** (Scheme 4) showed good larvicidal activity at concentrations < 140 ppm against *Aedes aegypti* larvae, whose mosquitoes are the major vector of dengue fever.[54]

It is believed that product yields could be increased by replacing the SSA catalyst with nanoordered MCM-41-SO₃H, which showed good to excellent results in such types of

reactions.[55] This MCM-41 functionalized with a grafted sulfonic acid group is easily prepared from MCM-41 and ClSO₃H in dichloromethane (Fig. 2B). The "pure" MCM-41 (S_{BET} = 991 m² g⁻¹) can be easily prepared from a template containing hexadecyl-trimethylammonium bromide, NH₃ solution, and tetraethylorthosilicate with final calcination at 550 °C.[56]

In 2012, Dekamin and Mokhtari[57] reported the use of MCM-41-SO₃H in the S-3CR process in ethanol for numerous and diverse α-amino nitrile series. Here, it was notable that this catalyst was used for at least five reaction cycles without significant loss of its activity. The MCM-41-SO₃H nanocatalyst also activates the formation of ald- and ketimines,[58] which are employed as versatile components in the asymmetric synthesis of α-amino nitriles and secondary amines.

A more complex silica boron sulfuric acid nanoparticle (SBSAN) catalyst allowed the efficient preparation of similar α-amino nitriles **5b** under solvent-free conditions at room
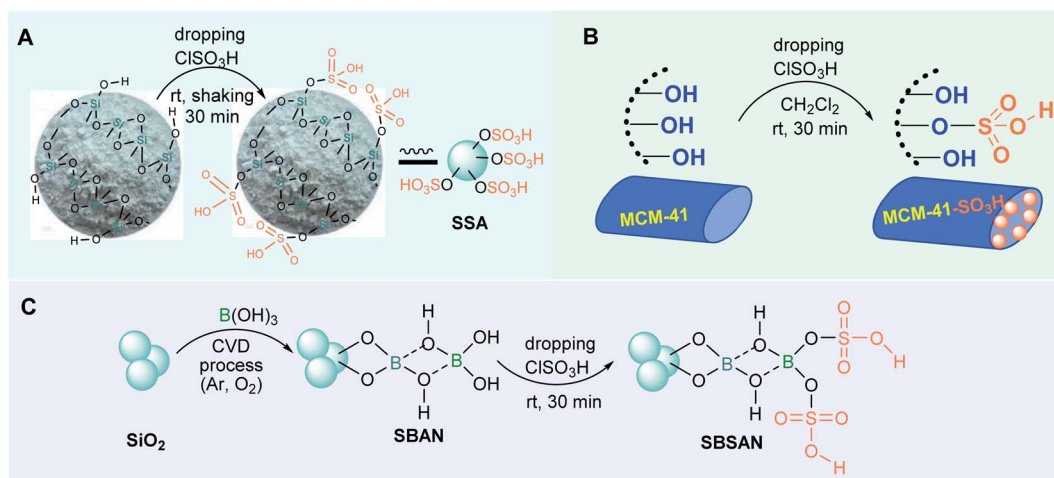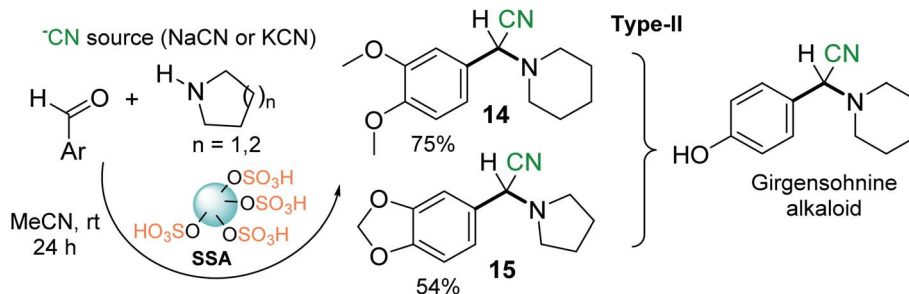

Fig. 2 Schematic representation of the heterogeneous acid nanocatalysts SSA (A), MCM-41-SO₃H (B), and SBSAN (C).

Scheme 4 SSA-catalyzed S-3-CR condensation is conducive to potential selective insecticides based on an α-amino nitrile skeleton.

temperature.[59] This constitutes a large advantage. However, this dual Brønsted/Lewis acid nanocatalyst is prepared in several steps starting with the alteration of the silica support by boric acid $B(OH)_3$ through the chemical vapor deposition (CVD) process and achieved with subsequent chlorosulfonic acid treatment (Fig. 2C).[60]

Siliceous mesoporous materials (silica gel or MCM-41) with Brønsted propylsulfonic acid groups were designed in the late 1990s[61,62] as recyclable solid acid catalysts. Applied as an alternative to traditional sulfonic resins, these materials quickly became especially popular acid catalysts for diverse kinds of chemical transformations. Propylsulfonic acid amorphous or/ and mesoporous silicas can be prepared from commercially available and inexpensive starting materials, such as (3-mercaptopropyl) trimethoxysilane (3-MPTS) or 3-((3-(trimethoxysilyl) propyl)thio)propane-1-sulfonic acid (3-TPTPSA). The complete covalent anchoring of 3-MPTS over silica is ensured during toluene reflux conditions to provide 3-mercaptopropyl-functionalized silica gel (MPS), a valuable material for the preparation of two types of propylsulfonic acid amorphous and mesoporous silicas, MCM-41-PSA[62,63] and silica-bonded *S*-sulfonic acid (SBSSA),[64,65] while the anchoring of 3-TPTPSA provides a 3-(propylthio)propane-1-sulfonic acid-functionalized

MCM-41 nanocatalyst (PTPSA@MCM-41 or MCM-41-PTSA)[66] (Scheme 5).

Silica-bonded 4-ethylphenylsulfonic acid (SBEPSA) can be obtained by tethering amorphous silica with trimethoxy(2-phenylethyl)silane (TPS) followed by sulfonation with chlorosulfonic acid (Scheme 5).[61] The latest developments in the preparation and application of similar and diverse sulfonic acid derivatives bonded to inorganic supports have been well reviewed by Niknam *et al.*[67] Currently, among the above-mentioned acid nanomaterials, only SBSSA was tested in S-3-CR condensation in ethanol at room temperature for 30 min, exhibiting high yields of α-amino nitriles, mild reaction conditions, and an excellent recycling capacity. However, only aldehydes and anilines or benzylamines were employed in synthetic screening.[68]

Other acid-functionalized mesoporous silica nanoparticles are based on sulfamic acid derivatives, such as silica-bonded *N*-propylpiperazine sulfamic acid (SBPPSA), and its homolog, silica-bonded *N*-propylhomopiperazine sulfamic acid (SBPHSA). Both materials are prepared *via* the sol–gel method from commercially available and inexpensive 3-chloropropyl-trimethoxysilane (3-CPTS), which is immobilized upon activated silica gel (with a surface area of 422 m² g⁻¹) by suspension
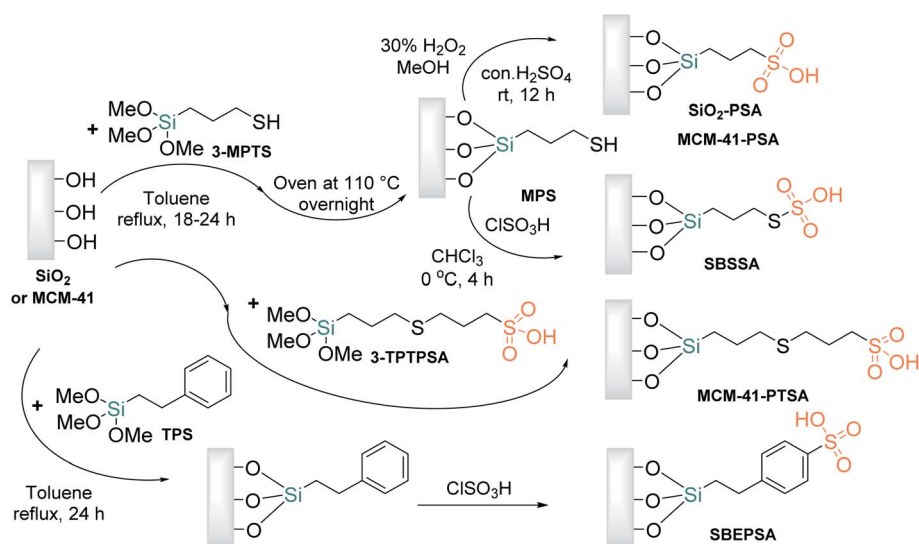
Scheme 5 Simplified representation of propylsulfonic acid silica preparation.
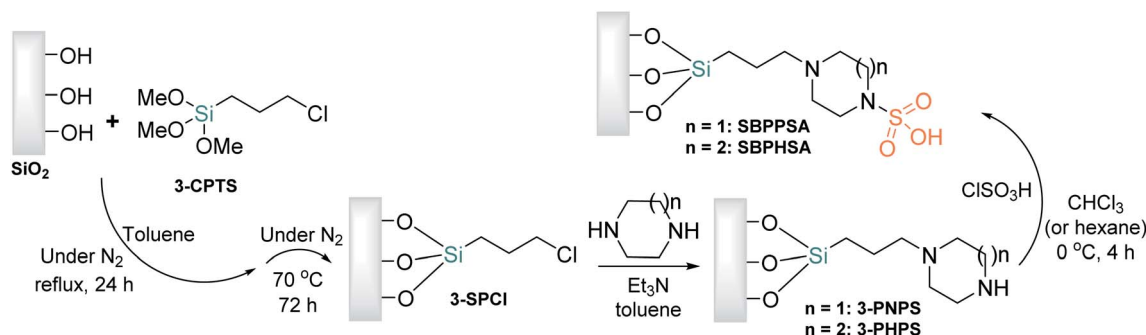
Scheme 6 Schematic representation of silica-bonded N-propyl(homo)piperazine sulfamic acid preparation.

in dry toluene or xylene.[69,70] The obtained organochlorine functional agent, 3-SPCl, is then treated with piperazine or homo piperazine at 60–70 °C in the presence of triethylamine as a proton abstractor under continuous stirring and a dry nitrogen atmosphere for 48 h to afford 3-(homo)piperazine-N-propylsilicas (3-PNPS or 3-PHPS), which react with chlorosulfonic acid in chloroform at 0 °C over 2 h, providing the respective SBPPSA and SBPHSA nanocatalysts as cream powders (Scheme 6).

Both prepared nanomaterials were tested as acid catalysts and proposed for S-3CR condensations.[70,71] SBPPSA-catalyzed Strecker reactions were performed in ethanol at room temperature for 5–50 min,[70] while the S-3-CRs catalyzed by SBPHSA were performed under solvent-free conditions for 10–30 min,[71] showing similar high efficiency in α-amino nitrile formation. From the point of sustainable synthesis, the best solvent is no solvent, *i.e.*, solvent-free processes are most desirable. Theoretically, these processes can remove the waste. According to the

selected results on the Strecker reactions in the presence of silica-bonded sulfonic acid-derived nanocatalysts (Table 3), three-component reaction processes under solvent-free conditions are considerably rapid and efficient.

Apparently, none of these propyl sulfonic acids for the S-3-CR condensations can generate first ketimines and then quaternary α-amino nitriles **12** (type IV), or at least, none were obtained in these experiments. Thus, current research and development for specific acid nanocatalysts could activate ketone components from S-3-CR condensations.

SBA-15 and its derivatives

SBA-15 (Santa Barbara amorphous) silica, synthesized by Stucky and coworkers in 1998,[72] is another mesoporous molecular sieve of industrial importance. Similar to MCM-41, SBA-15 possesses uniform hexagonally arrayed channels but with larger pore diameters (from 4 to 30 nm) and thicker pore walls[73] (Scheme 7A). This modified silica with an approximate surface

Table 3 Comparative analysis of the catalytic role of silica-bonded sulfonic acid derivatives

Nanocatalysts/solvents	9, Type-I	12, Type-IV	16, Type-I	17, Type-II
SSA /CH₂Cl₂, rt	91%, 7h	Not tested	91%, 4.5 h	84%, 8 h (X=N) 81%, 9 h (X=O)
MCM-41-SO₃H/EtOH, rt	98%, 30 min	Not tested	89%, 60 min	Not tested
SBSAN /solvent-free	96%,ᵃ 5 min	Not tested	Not tested	91%, 15 min (X=O)
SBSSA /EtOH, rt	92%,ᵃ 90 min	Not tested	Not tested	82%, 180 min (X=O)
SBPPSA /EtOH, rt	86%, 5 min	Not tested	Not tested	90%, 5 min (X=O)
SBPHSA /solvent-free	93%, 10 min	Not tested	90%, 15 min	Not tested

ᵃ Yields reported for *p*-toluidine derivatives.
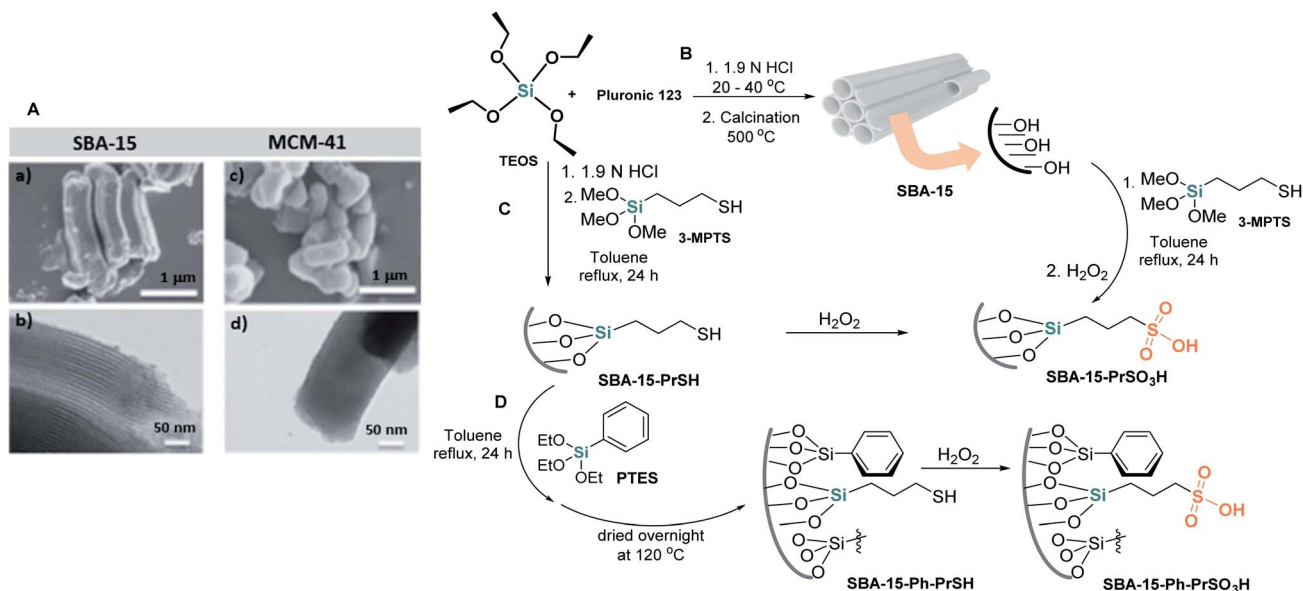
Scheme 7 (A) Images of the surface of SBA-15 ((a) SEM; (b) TEM) and MCM-41 ((c) SEM, (d) TEM). Reproduced from ref. 73 with permission from Oxford University Press, copyright [2020]. (B)–(D) Simplified representation of the synthesis of SBA-15 and its propylsulfonic acid analogs.

area of 800 m^2 g^{-1} is a promising support material for diverse chemical transformations.[74] Moreover, SBA-15 has much higher hydrothermal stability than MCM-41. Its common preparation consists of the interaction of tetraethoxysilane (TEOS) and SiO$_2$ as silicon sources and Pluronic 123 (EO$_{20}$PO$_{70}$EO$_{20}$, poly(-ethyleneoxide)–poly(propyl-enoxide)–poly(ethyleneoxide) block copolymer species) as a template, *i.e.*, the structure-directing agent, in an acid medium. The synthesis is a cooperative self-assembly process (Scheme 7B).

Similar to MCM-41, the internal surface of SBA-15 has been effectively altered by numerous organic functionalities or metallic species, and these modified SBA-15 silicas have been progressively designed and studied for use as carrier materials in drug delivery, adsorbents, sensors, or catalytic systems.[74,75] In this context, sulfonic-acid-functionalized mesoporous materials are promising acid catalysts,[76–78] and one of the most studied SBA-15 solid sulfonic acids, propylsulfonic acid functionalized SBA-15 (SBA-15-Pr-SO$_3$H), is not an exception. It was shown to be a highly powerful heterogeneous solid acid catalyst in diverse types of MCRs.[79]

Functionalizing SBA-15 with –SO$_3$H groups is usually performed through direct synthesis or postgrafting processes. The first procedure for SBA-15-PSA preparation was reported by Stucky and coworkers in 2000.[80] Their synthetic strategy was based on the cocondensation of TEOS and 3-MPTS in the presence of Pluronic P123 in acid media (1.9 M HCl) at room temperature. The resultant solution was stirred at 40 °C for 20 h, and then the mixture was aged at 100 °C for 24 h under static conditions. The solid (SBA-15-PrSH) was recovered by filtration and was air-dried at room temperature overnight. In the next step, this solid was oxidized with aqueous 30 wt% H$_2$O$_2$ at room temperature in an Argon atmosphere to create sulfonic moieties on the interior silica surfaces (Scheme 7C).

To obtain modified SBA-15-Pr-SO$_3$H with phenyl groups (SBA-15-Ph-Pr-SO$_3$H), Karimi and Zareyee treated SBA-15-Pr-SH with PhSi(OEt)$_3$ (PTES) in dry toluene to afford the corresponding SBA-15-Ph-Pr-SH, which was oxidized according to the Stucky protocol to obtain the desired sulfonic SBA-15 material (Scheme 7D).[81] This nanomaterial resulted in a more efficient catalyst in S-3CR condensation than SBA-15-Pr-SO$_3$H and successfully catalyzed this reaction of diverse ketones under solvent-free conditions to afford different and valuable quaternary α-amino nitriles **18** (types III and IV) (Scheme 8A).

Interestingly, the effectiveness of both SBA-15-Pr-SO$_3$H and SBA-15-Ph-Pr-SO$_3$H catalysts might depend on the pore size and hydrophobic character of these catalysts. Phenyl groups are in close proximity to sulfonic acid groups in SBA-15-Ph-Pr-SO$_3$H and decrease the affinity of the silica framework for water (byproduct reaction), allowing rapid desorption of the starting materials from the catalyst surface, while the SBA-15-Pr-SO$_3$H catalyst with a higher affinity for water retards the progress of the reaction.[81] Notably, the SBA-15-Ph-Pr-SO$_3$H catalyst with a 2D-hexagonal structure is highly stable and could be reused in fifteen successive runs with no significant loss of activity and with no considerable structural change (Scheme 8B). This green and cost-effective catalyst represents a useful alternative to the present procedures for scale-up hindered α-amino nitrile (*i.e.*, α-amino acid) preparation.

Pure siliceous Si-SBA-15 materials can also be modified by the incorporation of a high amount of Al into the framework of SBA-15. This alumination process is achieved through both one-step copolycondensation and postsynthesis methods.[82,83] The Al-SBA-15 material has both Lewis and Brønsted acid sites. Moreover, the acidity depends on the amount of aluminum incorporated into the siliceous framework. Kolli *et al.*[84] synthesized nanoporous heterogeneous Al-SBA-15 (*x*)-type aluminosilicate materials with different nSi/nAl ratios (*x* = 41,

Review
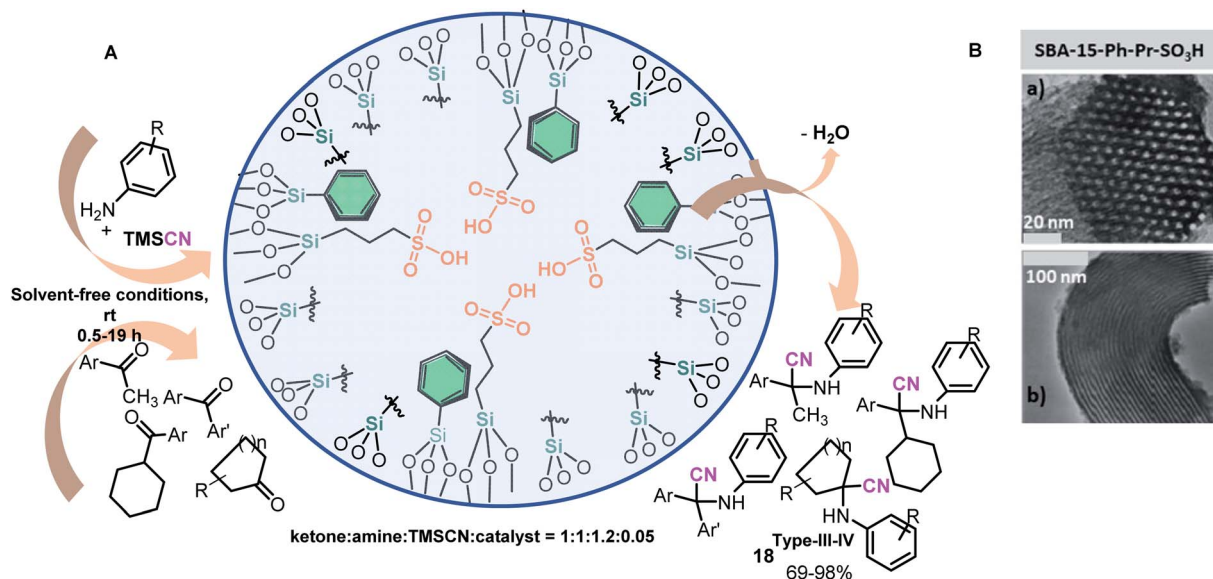
Scheme 8 (A) Solvent-free three-component Strecker reaction of ketones using an efficient and environmentally benign catalytic SBA-15-Ph-Pr-SO$_3$H system such as a nanoreactor. (B) TEM images of SBA-15-Ph-Pr-SO$_3$H nanocatalyst after the 15th reaction cycle: (a) perpendicular and (b) in the direction of the pore axis. Reproduced from ref. 81 with permission from the Royal Society of Chemistry, copyright [2009].

129, and 210) and specific surface areas ranging from 480 to 757 m^2 g^{-1} and tested these materials as catalysts for S-3-CR condensation. This little cited work yielded interesting results in my opinion. Performing the one-pot catalytic synthesis of diverse α-amino nitriles, including quaternary α-amino nitriles **19–20** (type III), in a water medium at room temperature (Scheme 9B), the authors noted that the Al content in the Al-SBA-15 catalyst considerably affects the product yields and reaction time.

The Al-SBA-15 catalyst with a Si/Al ratio of 41 was the best, which is due to the greater acidity of this catalyst in comparison to Al-SBA-15 (129) and Al-SBA-15 (210). The Al-SBA-15 material was prepared by optimizing the molar gel composition of aluminum isopropoxide, TEOS, and Pluronic 123 in deionized water in the presence of HCl stirring at 40 °C for 24 h and then aging at 100 °C for 48 h to obtain the crystallized product, which

was finally calcined at 550 °C for 36 h. Notably, the Al-SBA-15 catalyst, with a Si/Al ratio of 41, works well in the formation of α-amino nitriles **19–20**,[84] while the Al-MCM-41 catalyst fails in this precise case.[32]

Therefore, these developed methods could be considered one of the best for accessing diverse α-amino nitriles with quaternary amino groups incorporated in ketone skeletons as a powerful, green, and rapid synthesis. These methodologies are convenient for the scale-up process and tolerate a variety of functional groups and various electron-donating and electron-withdrawing groups with a wide substrate scope. However, it should be noted that the initial chemicals, above all, TEOS, are not as cheap as simple silica gel. Recently, sulfonic acid-functionalized Sn-SBA-15 catalysts were prepared by two different methods: one-step functionalization and post-functionalization. The obtained catalysts exhibited high
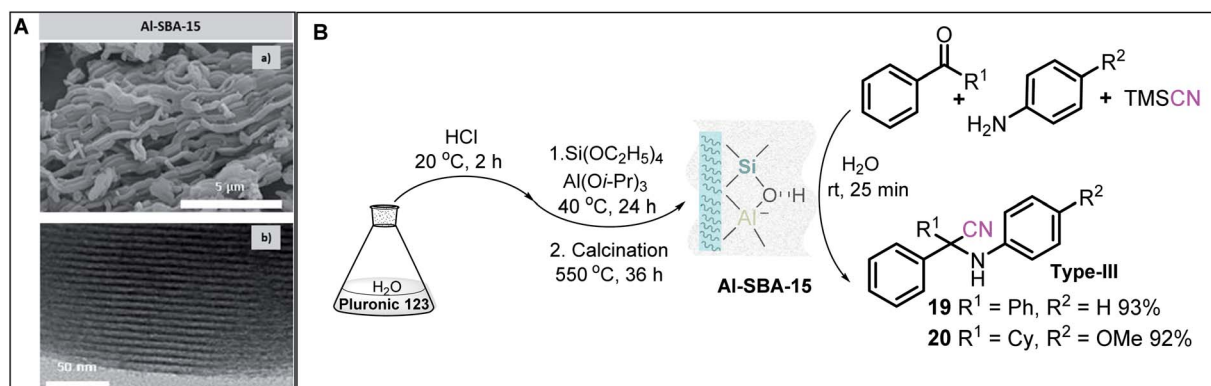
Scheme 9 (A) SEM image (a) and TEM image (b) of AlSBA-15 (41) sample. Reproduced from ref. 84 with permission from Elsevier, copyright [2017]. (B) Alumination process for Al-SBA-15 preparation and its use as a nanocatalyst in the S-3-CR of ketones, anilines, and TMSCN.

catalytic activity due to their high acidity.[85] We can only wait for someone to study them in the S-3-CR condensation.

Catalytic cycles of the S-3-CR in the presence of silica sulfuric acid ($SiO_2@SO_3H$) and MCM-41-SO_3H or SBA-15-Pr-SO_3H and its more complex analogs closely resemble those shown in Scheme 3A. All these catalysts activate the carbonyl group of aldehydes or ketones through hydrogen bonding for the nucleophilic attack of the amine to occur. Additionally, the presence of the catalyst can also activate the corresponding imine carbon for the posterior attack by the cyanide anion from TMSCN.[57,60,66]

Clay catalysts

Clays, a group of aluminosilicates, are widely used in many applications and exhibit specific features, such as acidity and proper surface properties. They are composed of multiple layers of polyhedrons, such as tetrahedral silicon oxides and octahedral hydrous alumina, where the layer spacing is approximately 1–2 nm and can be used directly in their natural form or after undergoing chemical or thermal treatments. Among them, cationic clay montmorillonite (MMT), a naturally abundant material (with mostly sodium ions, *i.e.*, Na-MMT, whose chemical composition is as follows: SiO_2, 63.0%; Al_2O_3, 16.2%; Fe_2O_3, 4.9%; CaO, 0.3%; MgO, 4.6%; Na_2O, 3.6%; K_2O, 0.1%; TiO_2, 0.4%), and its modified structures, such as K10 and KSF, are the most broadly employed acidic clays (both Brønsted and Lewis acid properties) in the field of clay-mediated organic synthesis. Their price is relatively low compared to other heterogeneous catalysts, and this combination of good properties and price makes them attractive catalysts for industrial applications.

Therefore, due to their noncorrosive properties, low cost, and ease of preparation, montmorillonite clays should be studied more and applied as catalysts in α-amino nitrile preparation. To date, there are a few examples of their use in S-3-CR condensation. MMT-K10 clay also successfully catalyzes the reaction of benzaldehydes, (S)-α-phenylethylamine, and NaCN in water in the presence of 1,6-bis(triphenylphosphonium)

hexane dibromide (P-6-P) as a phase transfer catalyst under ultrasonic irradiation to give diastereomeric mixtures of tertiary α-amino nitriles **21** (type I)[86] (Scheme 10A).

Yadav *et al.*[87] demonstrated for the first time the suitability of MMT-KSF in the condensation of aromatic aldehydes, anilines (or benzylamines), and TMSCN in CH_2Cl_2 at ambient temperature to afford the corresponding α-amino nitriles **22** (type I) in excellent yields (Scheme 10B). In addition, MMT-K10 clay promotes the microwave-assisted synthesis of a wide variety of α,α,α-trifluoromethylated ketimines from trifluoromethyl ketones and various amines at 175 °C (ref. 88) that can be used in tertiary α-amino nitrile preparation.

It is known that K10 and KSF clays derived from pristine Na-MMT, whose layered crystals aggregate into large particles (Scheme 11A),[89] differ in their surface area as well as in their acidity properties: whereas K10 montmorillonite possesses moderate acid strength (pH values of 3–4) and high surface area (220–270 $m^2\ g^{-1}$), KSF montmorillonite exhibits a more acidic character (pH value of 2.1) but less surface area (20–40 $m^2\ g^{-1}$). Thus, these two characteristics usually compete with each other, and it is difficult to select suitable reaction conditions for ideal S-3-CR condensation realization.

Nonetheless, Wang *et al.*[90,91] found a way out of this situation by preparing a Sn-MMT catalyst through the ion exchange of pristine Na-MMT with aqueous $SnCl_4$, which contained nanoparticles of SnO_2 intercalated between the silicate layers. The prepared catalyst possesses a higher specific surface area (280 $m^2\ g^{-1}$) than that of the pristine Na-Mont (12 $m^2\ g^{-1}$) and its modified abovementioned clays and possesses both strong Brønsted and Lewis acid sites in the montmorillonite interlayers. Due to these physical characteristics, a very small amount of Sn-MMT (10 mg; Sn: 1.9 mol%) could significantly increase the reaction rates of S-3-CR condensation at room temperature, particularly in the case of sterically hindered ketones, for quaternary α-amino nitrile **23** (type IV) preparation[91] (Scheme 11B).

Interestingly, in this case, the use of a solvent considerably delayed the Strecker reaction, while the solventless procedure
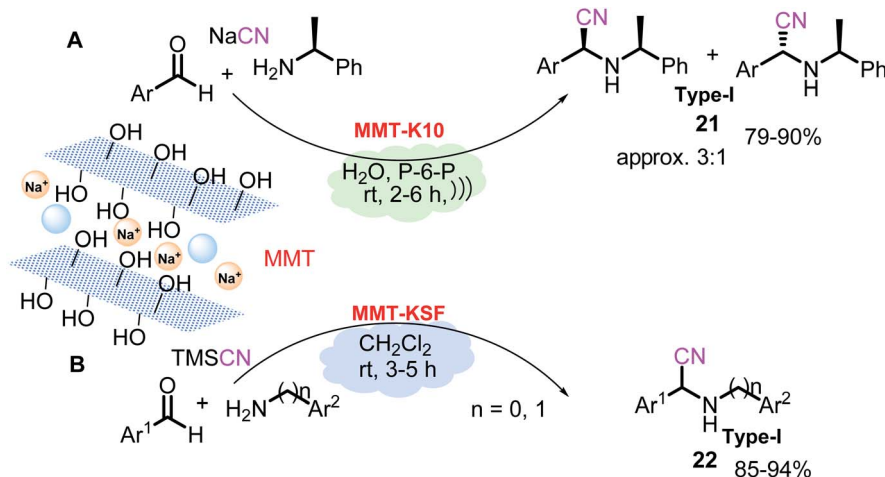
Scheme 10 Solvent-free, catalytic three-component Strecker reaction in the presence of modified MMT.
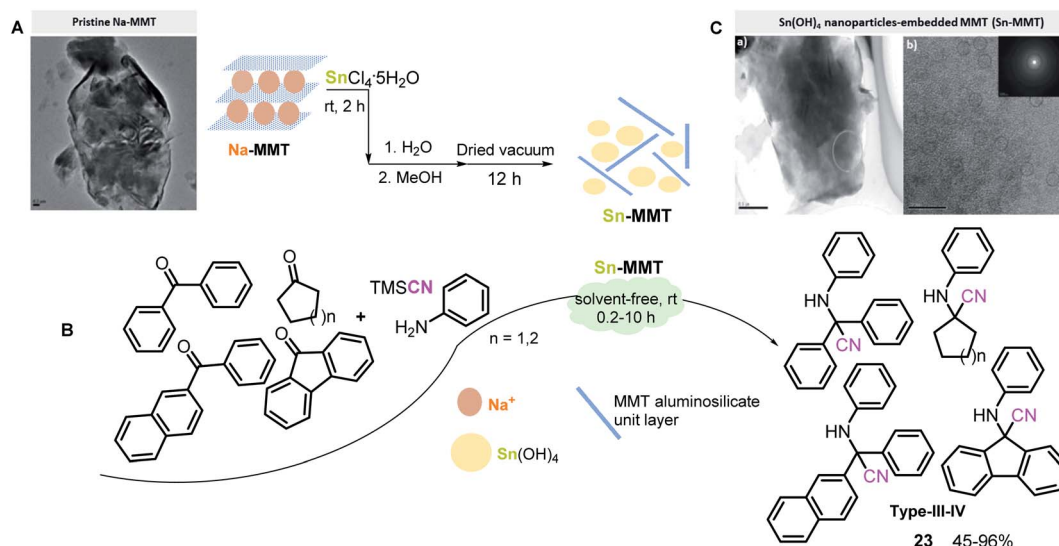
Scheme 11 (A) TEM image of pristine Na-MMT. Reproduced from ref. 89 with permission from MDPI, copyright [2013]. (B) Solvent-free preparation of ketone-based α-amino nitriles in the presence of a Sn–MMT nanocatalyst. (C) TEM images of $Sn(OH)_4$ nanoparticles-embedded MMT (Sn-MMT): (a) a low-resolution image; (b) a high-resolution image showing the lattice fringes of the $Sn(OH)_4$ nanoparticles in the dotted circles. Reproduced from ref. 92 with permission from Elsevier, copyright [2014].

afforded excellent results. Additionally, Sn-MMT was a better catalyst than its analogs, such as Al-MMT, Sn-MCM-41, and Al-MCM-41, with high specific surface areas and ordered mesopores. In 2014, the same Japanese scientific team guided by Onaka found the origin of Sn-MMT catalytic acid activity, discovering that Sn-MMT comprises $Sn(OH)_4$-based nanoparticles (nano-$Sn(OH)_4$) of less than 3 nm in diameter surrounded by delaminated MMT aluminosilicate unit layers, which means that Sn-MMT materials do not possess a typical laminated Na-MMT structure or the structure of pillared clays but can be a nanoporous composite of aluminosilicate layers and nano-$Sn(OH)_4$ (Scheme 11C).[92]

Finally, at the end of Section 1, it is necessary to mention that the three types of silicas discussed above can be easily functionalized by acidic ionic liquids, which exhibit remarkable properties such as nonflammability, negligible vapor pressure,

wide liquid range, and high thermal, chemical, and electrochemical stability and thus are used for a vast array of applications.[93] Nevertheless, their high cost, substantial consumption, and complicated recuperation affect much of their large-scale application. Therefore, chemical bonding grafting of ionic liquids on the surface of solid supports is a beneficial way to bring together the advantageous characteristics of ionic liquids and solid properties. Brønsted ionic liquids supported on mesoporous silicas and nanoporous Na⁺-MMT, such as SiO_2-[PIM]HSO_4,[94] SiO_2-[PIM-SO_3H]Cl,[95] SBA-15-[PMIM]Cl,[96] SBA-15-[PPIM-SO_3H]Br[97] and Na⁺-MMT-[PMIM]HSO_4 (ref. 98) (Fig. 3), are a good option to minimize process costs (reducing the amounts of ionic liquids) and improve synthetic protocols (facilitating their handling, separation, and reuse). Among them, only the heterogeneous silica-based ionic liquid SiO_2-[PIM]HSO_4 was used as a catalyst for the synthesis of
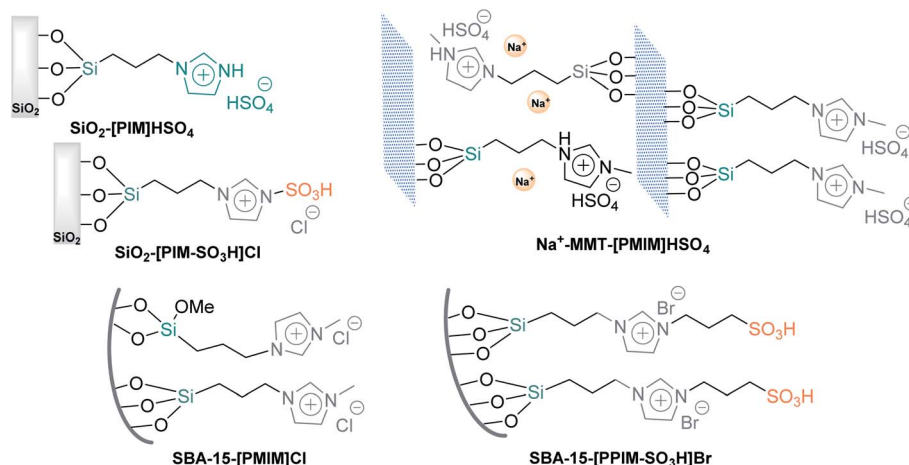

Fig. 3 Schematic representation of a Brønsted acidic ionic liquid supported on mesoporous silicas and nanopores and clays.

tertiary α-amino nitriles *via* the S-3-CR condensation of benz-aldehydes, amines, and trimethylsilyl cyanide in EtOH at room temperature.[94] The recovered catalyst was dried and recycled four times; however, it was not active in quaternary α-amino nitrile preparation.

Considering the results of Sn-MMT-catalyzed S-3-CR condensation (Scheme 11), it would be interesting to prepare and test the Sn-MMT-[PMIM]HSO$_4$ catalyst in this condensation with the same series of ketones. This last comment is also valid for the following catalysts couples: SiO$_2$-[PIM]HSO$_4$ and SiO$_2$-[PIM-SO$_3$H]Cl.

Mesoporous molecular sieve-supported metal complexes

With the same idea of improving and economizing on the chemical processes and reducing environmental impact, a silica matrix can also serve for the immobilization of catalytic complexes such as, for example, Schiff base derivatives, given that the covalent anchoring pathway allows the heterogeniza-tion of homogeneous catalysts. The grafting process of Schiff-base metal complexes onto the internal surface of silica gel or mesoporous silica type MCM-41 and SBA-15 through Si–O–Si bonds was reported 1996–1998.[99,100] These mesoporous silica-supported metal complexes catalysts, particularly salen Co(II) complexes, became very popular in organic trans-formations,[101,102] and in 2010, these catalysts were tested in the S-3-CR condensation when Rajabi *et al.*[103] reported that the SBA-15-salen-Co catalyst possessed the ability to efficiently catalyze the three-component Strecker reaction, obtaining tertiary α-amino nitriles **24** (type-II) at excellent yields at room tempera-ture under solvent-free conditions for 1–5 h, and preparation of quaternary α-amino nitriles **25** (types III and IV) was realized *via* the cyanation reaction of respective ketimines or ketiminium salts and TMSCN at 40 °C for 2.5–12 h (Scheme 12). This catalyst showed excellent recoverability and reusability over ten successive runs. The same authors demonstrated that the use of microwave irradiation conditions of these condensation

reactions significantly reduced reaction times (typically 30–45 min) at comparable temperatures (40–45 °C).[104] The SBA-15-salen-Co catalyst was prepared through a very simple grafting procedure. First, salicylaldehyde and 3-amino-propyltrimethoxysilane (3-APTMS) were mixed in absolute MeOH at room temperature to give an imine intermediate that forms a SiO$_2$(SBA-15)-salen-Co complex after the addition of cobalt(II) acetate to the reaction mixture. Prior to surface modification, nanoporous silicas were activated when added to concentrated HCl and subsequently washed with deionized water[105] (Scheme 12).

However, despite their high efficiency and activity, as well as their recyclability and low catalyst loading, these catalyst systems did not obtain further development for this vitally important reaction. This last statement also corresponds to morphology-controllable silica-based nanostructures with high specific surface areas, large pore volumes, and diverse silhou-ettes and architecture (vesicle-like, rod-like, cage-like struc-tures, tremella-like silica spheres, multi-shelled, hollow, or wrinkled nanoparticles, *etc.*).[106–111] Efforts in the preparation and functionalization of these innovative nanomaterials are very important tasks. Better understanding morphology control and studying their unique size-dependent catalytic behavior and cycle stability would allow us to fabricate new efficient and specific nanocatalysts with well-defined properties. There are inspiring and promising results: synthesis of multi-shelled mesoporous silica nanoparticles (MMSNs) through a dual-templating route (CTAB and sodium dodecyl benzene sulfo-nate as co-templates, and aqueous ammonia and TEOS) has been achieved. Furthermore, the Au-decorated MMSNs (Au@MMSNs) were assembled as the catalyst, which showed superior catalytic activity and good cycle stability for the reduction of 4-nitrophenol.[108] Wrinkled silica nanoparticles (WSNs) with controllable particle size (240 nm to 540 nm) and average pore size (7.4 nm to 10.1 nm), prepared *via* sol-vothermal synthesis using CTAB and polyvinylpyrrolidone, were used as carriers to immobilize *Candida rugosa* lipase (CRL). This prepared WSNs-CRL material revealed a good catalytic
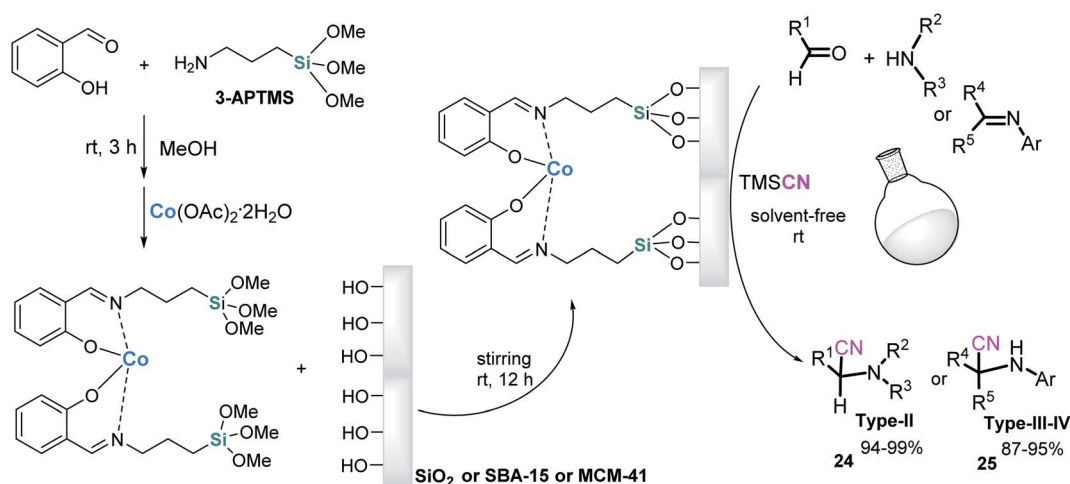
Scheme 12 Preparation of SBA-15-salen-co complex catalyst and its use in the S-3-CR condensation.

performance for the conversion of oleic acid (86.4%) through the esterification of oleic acid with methanol to prepare biodiesel.[111]

Fe$_3$O$_4$@SiO$_2$ core–shell nanoparticles

Among different classes of hybrid nanostructures, so-called core–shell nanoparticles,[112] magnetic nanoparticles of magnetite, a form of naturally occurring iron oxide, Fe$_3$O$_4$, that is embedded in the silica surface, are the most promising catalysts for chemical transformations.[24,113,114] The use of these magnetic nanocatalysts is a rapidly rising area for the progress of sustainable procedures. Magnetic separation not only precludes the need for catalyst filtration or centrifugation after completion of the reaction but also offers practical techniques for recovering these catalysts.[115] Therefore, a constant necessity for further and comprehensive research on magnetically recoverable multifunctional catalysts in a wide range of multicomponent reactions, including S-3-CR condensations, to develop more efficient and green chemical processes is quite evident.

Generally, this type of magnetic nanoparticle is readily accessible by different synthetic methodologies, including coprecipitation, sol–gel techniques, microemulsion, thermal decomposition, hydrothermal synthesis, sonolysis, and microwave irradiation.[115–118] Among them, sol–gel techniques based on the Stöber method and its modifications stand out as traditional, simple, and surfactant-free procedures that consist of coating iron oxide particles with uniform layers of silica by hydrolysis of TEOS in water, ammonia (ammonia hydroxide, NH$_4$OH), and 2-propanol mixtures through one-pot or two-step processes[118–121] (Scheme 13A). Naked Fe$_3$O$_4$ nanoparticles (NPs) are commonly prepared by chemical coprecipitation of Fe^{3+} and Fe^{2+} ions with a molar ratio of 2 : 1 (FeCl$_3$·6H$_2$O and FeCl$_2$·4H$_2$O, respectively) in deionized water at 85 °C under an N$_2$ atmosphere with vigorous mechanical stirring.

Then, 25% NH$_4$OH is rapidly added to the reaction mixture in one portion. The addition of the base to the Fe^{2+}/Fe^{3+} salt solution formed a black iron oxide magnetic nanoparticle

precipitate, which was treated to obtain a powder ready to be employed.

This "union" of Fe$_3$O$_4$ with SiO$_2$ is very beneficial for this couple from diverse points of view: physical and chemical stability, durability, toxicity, and surface functionalization possibility, all of which are undisputed advantages. As demonstrated above, silica is rich in surface hydroxyl groups, which provide simple, successful functionalization of Fe$_3$O$_4$ nanoparticles. Consequently, the easy postsynthetic functionalization of these hybrid materials can increase their synthetic application.[114] Noteworthy that the coating regulations of Fe$_3$O$_4$ NPs can produce the core/shell NPs with a single core and with different shell thicknesses, and it especially can be directed to different sizes Fe$_3$O$_4$ NPs and prevent the formation of core-free silica particles. For example, having an ethanol/hexane/oleic acid solvent mixture, the size of Fe$_3$O$_4$ NPs can be adjusted easily by modifying the reaction time and oleic acid content. To prepare the Fe$_3$O$_4$@SiO$_2$ core–shell NPs structure with a single core of 8.5 nm shell thickness, the optimal silica coating regulations (the proportion of Igepal CO-520 as a surfactant, ammonia, and TEOS) must be done[116] (Scheme 13B).

Following the logic of the previous sections, several sulfonated core–shell magnetic nanoparticles (Fig. 4) can be found in the chemical literature; they have already been employed as hydrophobic catalysts in various types of water-generating MCRs,[122–125] but their use as highly active, durable protonic acids and catalysts in S-3-CR condensation is still scarce and poorly studied and developed. It should be noted that the combination of both functionalities (acidic and hydrophobic) makes available a less polar organic environment with a relatively strong acidity for acid-catalyzed reactions.

Considering that the hydrophobic-hydrophilic balance on the catalyst surface and the acidity of the catalyst have a significant effect on the progress of S-3-CR condensation, which involves hydrophobic and hydrophilic substrates, Mobaraki et al.[126] developed an Fe$_3$O$_4$@SiO$_2$@Me&Et-PhSO$_3$H catalyst with water-resistant properties and studied it in the S-3-CR of ketones with amines (anilines and benzylamine) and TMSCN in a solvent-free environment at 60 °C. Noteworthy that TEM studies disclosed the core–shell structure of the nanoparticles with a diameter of ≈24 nm. Its use allowed to efficiently obtain a wide range of quaternary α-amino nitriles 26 (types III and IV) derived from alicyclic, strained cyclic, aliphatic, aromatic, or heteroaryl ketones (Scheme 14A).

Preparation of this catalyst encompasses common cocondensation reactions of 2-(4-chlorosulfonylphenyl)ethyl-trimethoxysilane (CSPETS) and trimethoxymethylsilane (TMMS) on silica-coated magnetic nanoparticles (Fe$_3$O$_4$@SiO$_2$) in dry toluene at room temperature.[127] High yields, the use of a green and magnetically separable heterogeneous catalyst, and its stability and low loading are the advantages of this work. However, the process developed is somewhat slow (1.5–30 h). Kassaee et al. demonstrated that another sulfonic heterogeneous catalyst, sulfamic acid-based magnetic iron oxide nanoparticles with a size distribution of 30–60 nm (average ≈ 40 nm), Fe$_3$O$_4$@SiO$_2$@PrNHSO$_3$H, also efficiently promotes the rapid formation of quaternary ketone-based α-amino nitriles 26
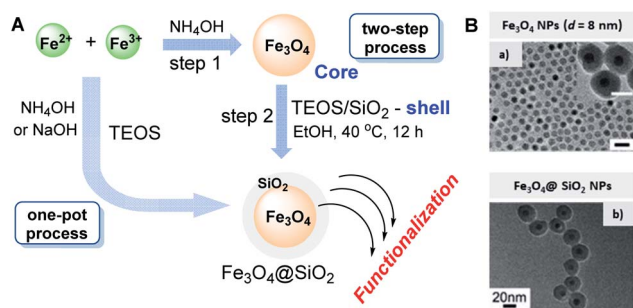
Scheme 13 (A) Sol–gel techniques based on the Stöber method through one-pot or two-step processes. (B) TEM images: (a) Fe$_3$O$_4$ NPs with sizes of 8.8 nm (scale bar = 20 nm), (b) Fe$_3$O$_4$@ SiO$_2$ core–shell NPs with Fe$_3$O$_4$ sizes of 8.8 nm and shell thickness of 8.5 nm. Reproduced from ref. 116 with permission from the American Chemical Society, copyright [2012].
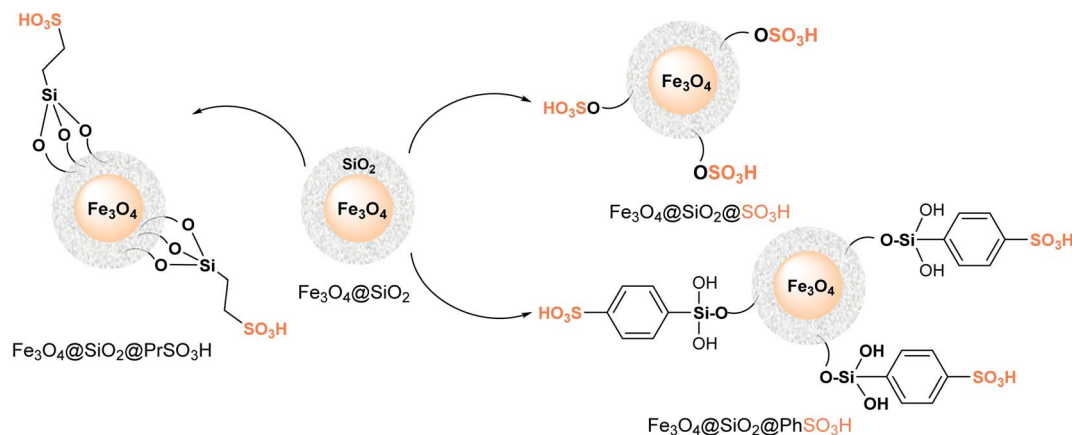
Fig. 4 Simplified structural representation of heterogenous sulfonated core−shell magnetic nanoparticle catalysts.

(types III and IV) in water at room temperature[128] (Scheme 14B). Notably, both hydrophobic magnetic solid sulfonic acid catalysts readily promote tertiary aldehyde-based α-amino nitrile formation at room temperature under solvent-free conditions.

It would be interesting to probe additional types of sulfonic heterogeneous "mixed" catalysts, such as $Fe_3O_4@SiO_2$-based ionic liquid PIM/trinitromethane[129] or $Fe_3O_4@SiO_2$-based ionic liquid PIMB-SO$_3$H,[130] in α-amino nitrile preparation using S-3-CR condensation. On the other hand, different acid heterogeneous "hybrid" catalysts have recently been prepared and studied in MCR processes. Among them, $Fe_3O_4@SiO_2@$-PrNH-GA composite, amino-functionalized silica-based magnetic nanoparticles grafted with gallic acid (GA) resulted in an interesting green nanocatalyst for the S-3-CR condensation; however, the authors limited themselves to studying the reactions of aldehydes, aromatic amines, and TMSCN in ethanol at

room temperature, rapidly obtaining tertiary α-amino nitriles 27 (type I)[131] (Scheme 15).

The synthesis of this composite is based on a common method of Fe_3O_4 functionalization[132] as well as $Fe_3O_4@SiO_2@$-PrNHEt-OP(O)(OH)$_2$ nanocatalysts.[133] A layer of SiO_2 is anchored on the surface of the Fe_3O_4 nanoparticles by reaction with TEOS to form $Fe_3O_4@SiO_2$, which reacts with 3-chloropropyl trimethoxysilane $Fe_3O_4@SiO_2@$PrCl material in ethanol and deionized water to give the needed nanocatalyst, while a homogenous mixture of GA in dry toluene is added to the $Fe_3O_4@SiO_2@$-PrNH$_2$ precursor in the presence of ZrCl$_4$ as a cocatalyst resulting in the desired catalyst (Scheme 15).

Interestingly, Jafarzadeh et al.[134] demonstrated that $Fe_3O_4@SiO_2@$PrNH$_2$-supported trifluoroacetic acid (CF$_3$COOH, TFA), $Fe_3O_4@SiO_2@$PrNH$_2$·TFA works well as a nanocatalyst in the S-3-CR condensation of aldehydes (or ketones), amines, and sodium cyanide (but not TMSCN) in ethanol at room
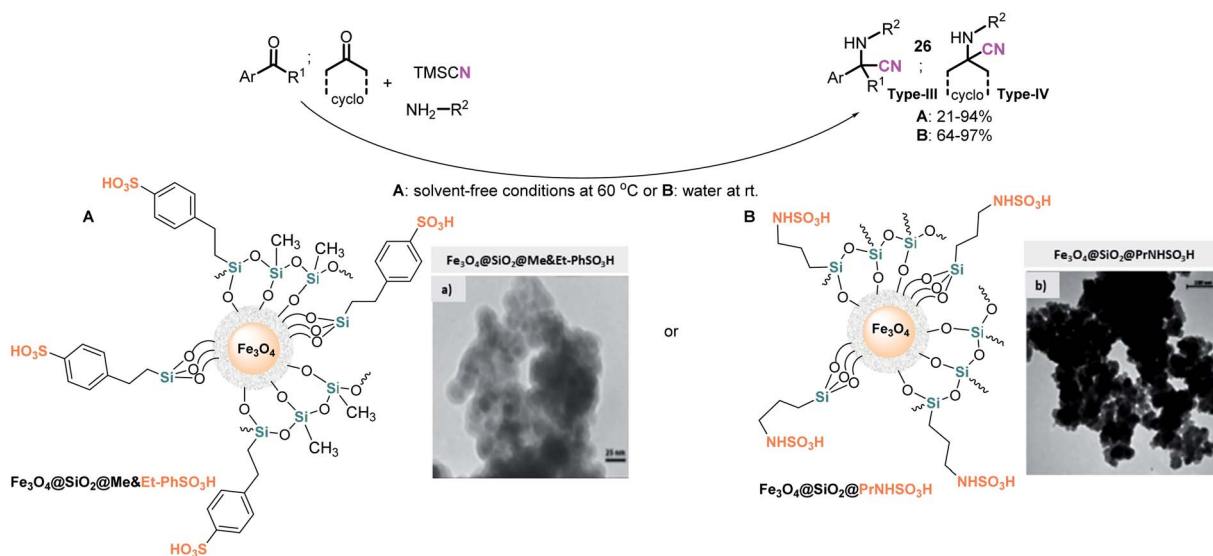
Scheme 14 Use of hydrophobic magnetic solid sulfonic acid catalyst in the S-3-CR of ketones with amines and TMSCN: (A) $Fe_3O_4@SiO_2@$-Me&Et-PhSO$_3$H catalyst and its TEM image (a) reproduced from ref. 124 with permission from Elsevier, copyright [2014]. (B) $Fe_3O_4@SiO_2@$-PrNHSO$_3$H catalyst and its TEM image (b) reproduced from ref. 123 with permission from John Wiley and Sons, copyright [2014].
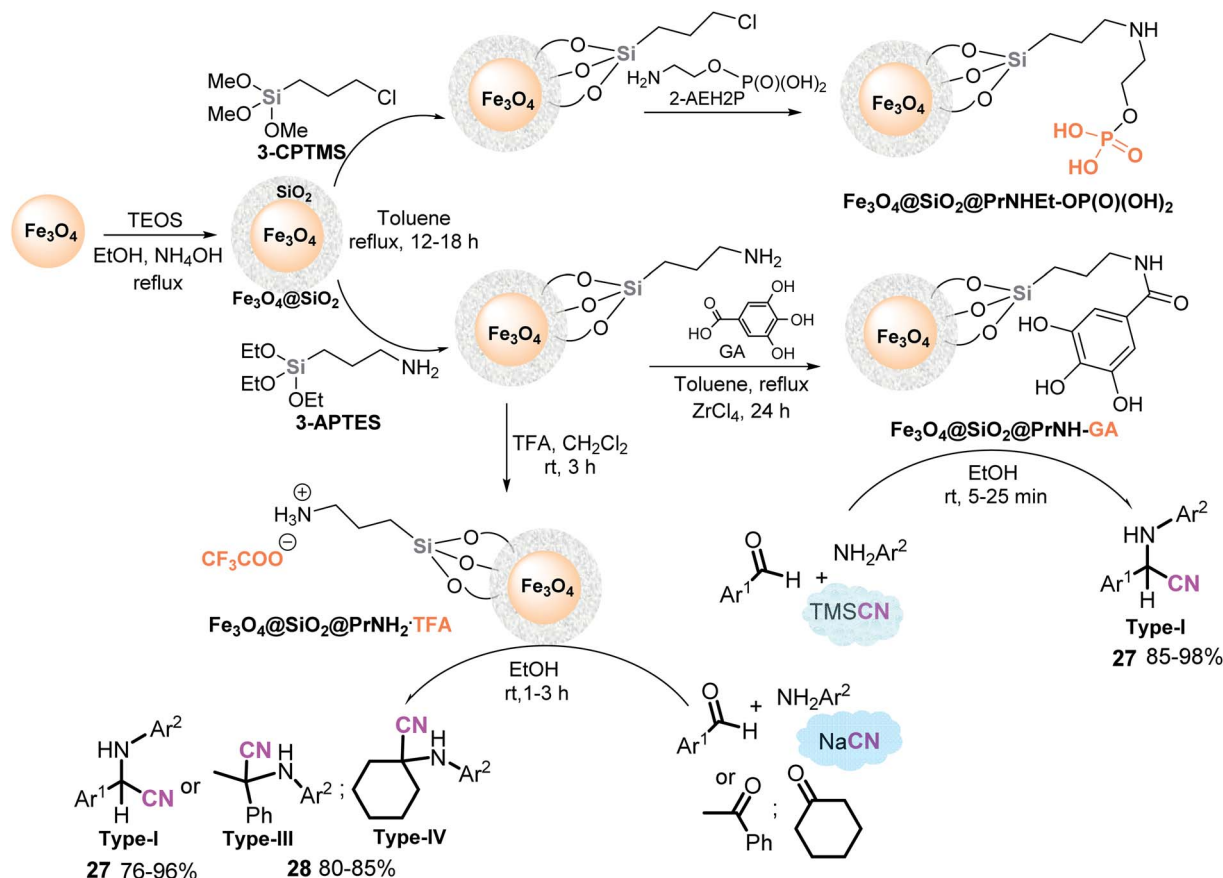
Scheme 15 Preparation of acid heterogeneous "metal–organic fragment mixed" catalysts and their use in the S-3-CR condensation.

temperature to afford the respective tertiary or quaternary α-amino nitriles 27–28 (types I, III and IV). Synthesis of proper Fe$_3$O$_4$@SiO$_2$@PrNH$_2$·TFA nanocatalyst is very simple and consists of the treatment of Fe$_3$O$_4$@SiO$_2$@PrNH$_2$ with TFA in CH$_2$Cl$_2$ at room temperature[135] (Scheme 15). Due to the simplicity of preparation and catalyst nature, the use of this nanomaterial seems to be important for increasingly efficient green chemical synthesis,[136] including Strecker-type reactions, considering that the Ziegler method for the isolation of anhydrous HCN (from an aqueous solution of NaCN or KCN and mineral acid) is still the main approach applied today for preparing anhydrous HCN on the laboratory scale.[137] In this context, Jafarzadeh's procedure should be studied more. Despite trimethylsilylcyanide (TMSCN) as a gaseous HCN surrogate being easier and safer to handle than HCN due to its higher boiling point, the most commonly used cyanide shows poor atom economy, high cost per mol, high toxicity, and potentially different reactivity than HCN.[138]

Combining the ideas of items 4 and 5, *i.e.*, the building of magnetic nanomaterials and metal complexes, several examples can be found. Fe$_3$O$_4$@Im[CN]Cu(II) complex nanocomposites,[139] Pd-MDA-PSi-Fe$_3$O$_4$ magnetic nanoparticles,[140] and Fe$_3$O$_4$@SiO$_2$@MoSB metal complexes[141] were prepared through multistep schemes and applied in the S-3CR

condensation of aldehydes, amines, and TMSCN but without significant improvements for α-amino nitrile preparation.

Asymmetric S-3-CR condensations under nanocatalysis?

Both study objects discussed in this work, S-3-CRs and nanocatalysts, are deeply involved in the hypothetical abiogenesis process of the origin of life. The prebiotic process is still not clear. Strecker reactions provide α-amino nitriles, which seem to be prebiotic α-amino acid precursors and thus can serve as peptide precursors, bringing an increase in chemical complexity.[142–144] These peptide precursors could be formed through α-amino nitrile ligation in water[145,146] or under mechanical, dynamic processes in the absence of water.[147] On the other hand, clay-organic materials, especially MMT, were spontaneously formed in nature and presumably could play a crucial role in these processes as catalysts or promoters[148] acting as "inorganic enzymes,"[22] or "molecular replicators".[149] Obviously, the chiral stereoselectivity process in this way of life is the key point.[150,151] Fruitful asymmetric Strecker reactions and, thus, optically active α-amino nitriles and proteinogenic and nonproteinogenic α-amino acids can be achieved through two general strategies: (1) the nucleophilic addition of cyanide to chiral nonracemic imines and (2) the catalytic

enantioselective cyanation of achiral imines. There have been huge advances in these strategies.[152–154]

Notably, the second approach is considered more suitable and promising for large-scale and industrial use. Several chiral Brønsted acids, Lewis bases, catalytic metal systems (Al, Ti, Zr, lanthanide compounds, *etc.*), phase-transfer catalysts, and chiral organo-catalytic systems (guanidines, ureas, thioureas, bisformamides, bis-(*N*-oxides), ammonium salts, *etc.*) are now available.[155,156] Although the use of these chiral molecular catalysts has achieved great success, in recent years, nano-structures have emerged as potential materials for asymmetric synthesis.[157,158] According to the above synthetic technique for hybrid SiO_2-based nanomaterials, diverse molecules, which contain chiral groups or are combined with metals or chiral complexes, can be anchored onto the external surface of amorphous silica or silica-aluminum through reaction with accessible silanol groups. In this way, the first hybrid enantio-selective catalysts were designed, generated, and studied for some organic transformations, such as the asymmetric hydrogenation of certain unsaturated compounds[159] and α-alkylation reactions,[160] 1,3-dipolar cycloaddition reactions[161] or asymmetric multicomponent reactions (*i.e.*, Michael-type condensation).[162] Unfortunately, these examples of chiral solid materials are still limited. Nevertheless, in the case of S-3-CR condensation, no catalyst has been developed thus far. It is believed that the studies realized by Feng *et al.*[160] or Safaei-Ghomi and Zahedi,[163] in which silica gel-supported cinchona alkaloid-based quaternary ammonium salt and L-proline-functionalized Fe_3O_4 nanoparticles have been prepared, respectively, could be very useful in search of this type of specific catalysts for the Strecker reaction.

Can the appearance of a chiral nanocatalyst that is active in the Strecker reaction be expected in the near future? Yes, without a doubt. The results accumulated during the last ten years on this topic give us new ideas and allow us to design innovative nanocatalysts that show high stereocontrol in asymmetric catalytic procedures, in addition to green and sustainable aspects of organic chemistry.

Conclusion and outlook

Nanocatalysis, which closes the gap between both conventional homogenous and heterogeneous catalysis, is a very particular and promising area with the awesome development of nanomaterials, *i.e.*, nanoparticles and nanocatalysts. The smaller size provides a high surface area per unit volume, making the nanocatalyst unique and more efficient. Compared to traditional catalysts, nanocatalysts reveal exceptionally enhanced catalytic activity, selectivity, durability, and recoverability. All these characteristics play a pivotal role in solving current environmental industrial problems, especially in the field of organic chemistry, which is based on organic reactions and transformations related to multicomponent reactions, including Strecker-type reactions that can offer diverse α-amino nitriles, which are valuable bifunctional building blocks in organic synthesis, medicinal chemistry, drug research, and organic materials science. Driven by green chemistry principles, the demand for sustainable and

safe chemical processes has promoted the use of alternative green solvents or even solvent-free conditions and balanced environmental nanocatalysts that all feature reduced environmental risk, reduced toxicity, cost-effectiveness, and reusability properties as the major advantages.

Over the past few years, ever-growing progress has been made in the synthesis of well-defined nanostructured materials as active heterogeneous catalysts for S-3-CR condensations. Among these materials, mesoporous silica sieves are the most studied nanoobjects due to their stable pore structure, easy preparation, and straightforward chemical manipulation in the functionalization process. Much progress has been made, but many challenges remain. Numerous kinds of structural types of nanocatalysts based on silicious materials have been designed and proposed, from tubular to bead passing with laminar structures. The use of several acid nanocatalysts, such as tubular SBA-15-Ph-Pr-SO_3H nanocatalyst, $Fe_3O_4@SiO_2@Me\&Et$-$PhSO_3H$, or $Fe_3O_4@SiO_2@PrNHSO_3H$ nanobead catalysts, allows the rapid formation of quaternary ketone-based α-amino nitriles, which are hardly available through conventional catalytic Strecker-type reactions. These nanocatalysts, especially silica-coated magnetic nanoparticles, are more attractive and will be appealing in the near future due to their high activity and selectivity, ready separation, and recyclable features.

However, their fabrication needs some improvements in terms of addressing green aspects. The obtention of high-performance catalysts or supports under environmental conditions is not a more important task than the preparation of desired α-amino nitriles or their derivatives needed for pharmaceuticals, drug discovery, and organic materials chemistry. Thus, in this stage of constant development of nanocatalysts and their application in various processes for the chemical industry, it is necessary to continue to study the possibility of nanocatalysis synthesis as well as the needed chemical production with the participation of proper catalysts actively involving the use of alternate energy inputs (*i.e.*, microwave and ultrasonic irradiations, visible light irradiation or mechanochemical mixing) or practices such as microflow techniques, *i.e.*, the use of microfluidic devices for continuous flow synthesis. The latter represents a highly useful and increasingly popular method suitable for organic processes based on multicomponent reactions, and it is believed that the combination of nanocatalysis and these innovative inputs and techniques will enrich and increase our scientific knowledge to another level in the frontier areas.[164]

The selected model reaction to study the nanocatalyzed S-3-CR condensation of benzaldehyde, aniline, and TMSCN is very simple and does not indicate the catalytic activity of the employed nanocatalyst and thus needs some corrections. This model reaction might include ketone components, such as acetophenone or cyclohexanone, and other cyanide sources or cyanation agents, which must be nontoxic components.[165] Suitable candidates for this casting would be potassium ferrocyanide ($K_4[Fe(CN)_6]$) and potassium ferricyanide ($K_3[Fe(CN)_6]$), both of which are available, simple, stable, and inexpensive nontoxic cyanide sources.[166] These latter cyanide components are also used in nucleophilic aromatic cyanation reactions as

well as oxidative α-cyanation reactions. It is interesting to note that these cyanoferrate complexes have also been proposed as prebiotic cyanide sources, *i.e.*, HCN surrogates, and Hernández *et al.*[167] demonstrated that the S-3-CR condensation of aldehydes, amines, and cyanoferrate complexes under mechanochemical activation conditions using ball milling results in the formation of α-amino nitriles, a chemical process related to early Earth conditions. In this context, the design and development of modern chiral nanocatalysts are of the utmost importance.

Finally, the guiding principles of green chemistry mentioned above are crucial to achieving the five R (R5) concepts (reduce, reuse, repurpose, recycle, and recover) for the development of circular organic chemistry.[168,169] In this context, the described silicious-based nanocatalysts would be ideal, indispensable, and very valuable players in this transition period to the circular process, which requires the sustainable production of both chemicals and efficient nanocatalysts.

Author contributions

Vladimir V. Kouznetsov: conceptualization, methodology, writing – original draft, review. José G. Hernández: formal analysis, copyright acquisition, review & editing.

Conflicts of interest

The author confirms that this article's content has no conflict of interest.

Acknowledgements

References

1 C. Grundke, N. Vierengel and T. Opatz, *Chem. Rec.*, 2020, **20**, 989–1016.

2 E. Ruijter and R. V. A. Orru, *Drug Discovery Today: Technol.*, 2013, **10**, e15–e20.

3 C. Lamberth, *Bioorg. Med. Chem.*, 2020, **28**, 115471.

4 L. Levi and T. J. Müller, *Chem. Soc. Rev.*, 2016, **45**, 2825–2846.

5 R. C. Cioc, E. Ruijter and R. V. A. Orru, *Green Chem.*, 2014, **16**, 2958–2975.

6 R. Schlögl and S. B. Abd Hamid, *Angew. Chem., Int. Ed.*, 2004, **43**, 1628–1637.

7 R. Schlögl, *Angew. Chem., Int. Ed.*, 2015, **54**, 3465–3520.

8 A. T. Bell, *Science*, 2003, **299**, 1688–1691.

9 M. Boudart, A. Aldag, J. E. Benson, N. A. Dougharty and C. Girvin Harkins, *J. Catal.*, 1966, **6**, 92–99.

10 X. Lim, *Nature*, 2016, **537**, 156–158.

11 V. Polshettiwar and R. S. Varma, *Green Chem.*, 2010, **12**, 743–754.

12 M. Kaushik and A. Moores, *Curr. Opin. Green Sustainable Chem.*, 2017, **7**, 39–45.

13 R. S. Varma, *ACS Sustainable Chem. Eng.*, 2016, **4**, 5866–5878.

14 V. V. Kouznetsov and C. E. P. Galvis, *Tetrahedron*, 2018, **74**, 773–810.

15 J. D. Sutherland, *Nat. Rev. Chem.*, 2017, **1**, 0012.

16 N. Kitadai and S. Maruyama, *Geosci. Front.*, 2018, **9**, 1117–1153.

17 R. Pascal and I. A. Chen, *Nat. Chem.*, 2019, **11**, 763–764.

18 K. B. Muchowska and J. Moran, *Science*, 2020, **370**, 767–768.

19 J. Hu, L. Chen and R. Richards, in *Metal Oxide Catalysis*, ed. S. Jackson and J. Hargreaves, Wiley-VCH Verlag GmbH & Co., Weinheim, Germany, 2008, pp. 613–663.

20 Y. Li, N. Kitadai and R. Nakamura, *Life*, 2018, **8**, 46.

21 V. Erastova, M. T. Degiacomi, D. G. Fraser and H. C. Greenwell, *Nat. Commun.*, 2017, **8**, 2033.

22 A. Rimola, M. Sodupe and P. Ugliengo, *Life*, 2019, **9**, 10.

23 H. C. Zeng, *Acc. Chem. Res.*, 2012, **46**, 226–235.

24 M. N. Chen, L. P. Mo, Z. S. Cui and Z. H. Zhang, *Curr. Opin. Green Sustainable Chem.*, 2019, **15**, 27–37.

25 M. B. Gawande, R. Zboril, V. Malgras and Y. Yamauchi, *J. Mater. Chem. A*, 2015, **3**, 8241–8245.

26 U. Ashik, A. Viswan, S. Kudo and J. Hayashi, in *Applications of Nanomaterials*, ed. S. Bhagyaraj, O. Oluwafemi, N. Kalarikkal and S. Thomas, Woodhead Publishing, Elsevier, Sawston, UK, 2018, pp. 45–82.

27 G. Martínez-Edo, A. Balmori, I. Pontón, A. Martí del Rio and D. Sánchez-García, *Catalysts*, 2018, **8**, 617.

28 C. T. Kresge, M. E. Leonowicz, W. J. Roth, J. C. Vartuli and J. S. Beck, *Nature*, 1992, **359**, 710–712.

29 R. Martínez, D. J. Ramón and M. Yus, *Tetrahedron Lett.*, 2005, **46**, 8471–8474.

30 B. Nammalwar, C. Fortenberry and R. A. Bunce, *Tetrahedron Lett.*, 2014, **55**, 379–381.

31 M. Eslami, M. G. Dekamin, L. Motlagh and A. Maleki, *Green Chem. Lett. Rev.*, 2018, **11**, 36–46.

32 K. Iwanami, H. Seo, J. C. Choi, T. Sakakura and H. Yasuda, *Tetrahedron*, 2010, **66**, 1898–1901.

33 R. Ryoo and J. M. Kim, *J. Chem. Soc., Chem. Commun.*, 1995, 711–712.

34 J. M. Kim, J. H. Kwak, S. Jun and R. Ryoo, *J. Phys. Chem.*, 1995, **99**, 16742–16747.

35 G. A. Eimer, L. B. Pierella, G. A. Monti and O. A. Anunziata, *Catal. Commun.*, 2003, **4**, 118–123.

36 Z. Y. Yuan, S. Q. Liu, T. H. Chen, J. Z. Wang and H. X. Li, *J. Chem. Soc., Chem. Commun.*, 1995, 973–974.

37 D. Q. Khieu, D. T. Quang, T. D. Lam, N. H. Phu, J. H. Lee and J. S. Kim, *J. Inclusion Phenom. Macrocyclic Chem.*, 2009, **65**, 73–81.

38 J. S. Choi, S. S. Yoon, S. H. Jang and W. S. Ahn, *Catal. Today*, 2006, **111**, 280–287.

39 M. T. Bore, R. F. Marzke, T. L. Ward and A. K. Datye, *J. Mater. Chem.*, 2005, **15**, 5022–5028.

40 Z. Derikvand and F. Derikvand, *Chin. J. Catal.*, 2011, **32**, 532–535.

41 A. Sayari, I. Moudrakovski, C. Danumah, C. I. Ratcliffe, J. A. Ripmeester and K. F. Preston, *J. Phys. Chem.*, 1995, **99**, 16373–16379.

42 M. G. Dekamin, Z. Mokhtari and Z. Karimi, *Sci. Iran.*, 2011, **18**, 1356–1364.

43 L. F. Chen, L. E. Noreña, J. Navarrete and J. A. Wang, *Mater. Chem. Phys.*, 2006, **97**, 236–242.

44 A. S. Golezani, A. S Fateh and H. A. Mehrabi, *Prog. Nat. Sci.: Mater. Int.*, 2016, **26**, 411–414.

45 M. A. Gonzales, H. Han, A. Moyes, A. Radinos, A. J. Hobbs, N. Coombs, S. R. J. Oliver and P. K. Mascharak, *J. Mater. Chem. B*, 2014, **2**, 2107–2113.

46 W. Y. Chen and J. Lu, *Synlett*, 2005, 2293–2296.

47 P. Salehi, M. Ali Zolfigol, F. Shirini and M. Baghbanzadeh, *Curr. Org. Chem.*, 2006, **10**, 2171–2189.

48 M. Gawande, R. Hosseinpour and R. Luque, *Curr. Org. Synth.*, 2014, **11**, 526–544.

49 R. Vekariya and H. Patel, *Arkivoc*, 2015, **2015**, 70–96.

50 H. Sepehrmansourie, *Iran. J. Catal.*, 2020, **10**, 175–179.

51 A. Pramanik and S. Bhar, *New J. Chem.*, 2021, **45**, 16355–16388.

52 M. A. Zolfigol, *Tetrahedron*, 2001, **57**, 9509–9511.

53 H. A. Oskooie, M. M. Heravi, A. Sadnia, F. Jannati and F. K. Behbahani, *Monatsh. Chem.*, 2008, **139**, 27–29.

54 A. L. Carreño Otero, L. Y. Vargas Méndez, J. E. Duque and V. V. Kouznetsov, *Eur. J. Med. Chem.*, 2014, **78**, 392–400.

55 R. H. Vekariya, N. P. Prajapati and H. D. Patel, *Synth. Commun.*, 2016, **46**, 1713–1734.

56 E. Vrbková, E. Vyskočilová and L. Červený, *React. Kinet., Mech. Catal.*, 2015, **114**, 675–684.

57 M. G. Dekamin and Z. Mokhtari, *Tetrahedron*, 2012, **68**, 922–930.

58 E. Ali, M. R. Naimi-Jamal and M. G. Dekamin, *Sci. Iran.*, 2013, **20**, 592–597.

59 A. Khalafi-Nezhad, H. O. Foroughi, M. M. Doroodmand and F. Panahi, *J. Mater. Chem.*, 2011, **21**, 12842–12851.

60 A. Khalafi-Nezhad, H. O. Foroughi and F. Panahi, *Heteroat. Chem.*, 2012, **24**, 1–8.

61 R. D. Badley and W. T. Ford, *J. Org. Chem.*, 1989, **54**, 5437–5443.

62 W. D. Bossaert, D. E. De Vos, W. M. Van Rhijn, J. Bullen, P. J. Grobet and P. A. Jacobs, *J. Catal.*, 1999, **182**, 156–164.

63 S. Shylesh, S. Sharma, S. P. Mirajkar and A. P. Singh, *J. Mol. Catal. A: Chem.*, 2004, **212**, 219–228.

64 K. Niknam, D. Saberi and M. N. Sefat, *Tetrahedron Lett.*, 2009, **50**, 4058–4062.

65 S. Safaei, I. Mohammadpoor-Baltork, A. R. Khosropour, M. Moghadam, S. Tangestaninejad and V. Mirkhani, *J. Iran. Chem. Soc.*, 2017, **14**, 1583–1589.

66 K. Niknam, H. Hashemi, M. Karimzadeh and D. Saberi, *J. Iran. Chem. Soc.*, 2020, **17**, 3095–3178.

67 K. Niknam, D. Saberi and M. N. Sefat, *Tetrahedron Lett.*, 2010, **51**, 2959–2962.

68 R. K. Dey, T. Patnaik, V. K. Singh, S. K. Swain and C. Airoldi, *Appl. Surf. Sci.*, 2009, **255**, 8176–8182.

69 Z. Nasresfahani, M. Z. Kassaee and E. Eidi, *New J. Chem.*, 2016, **40**, 4720–4726.

70 T. Rahi, M. Baghernejad and K. Niknam, *Chin. Chem. Lett.*, 2012, **23**, 1103–1106.

71 Z. Nasresfahani, M. Z. Kassaee and E. Eidi, *J. Iran. Chem. Soc.*, 2019, **16**, 1819–1825.

72 D. Zhao, J. Feng, Q. Huo, N. Melosh, G. H. Fredrickson, B. F. Chmelka and G. D. Stucky, *Science*, 1998, **279**, 548–552.

73 P. Muchan, C. Saiwan and M. Nithitanakul, *Clean Energy*, 2020, **4**, 120–131.

74 J. A. S. Costa, R. A. De Jesus, D. O. Santos, J. B. Neris, R. T. Figueiredo and C. M. Paranhos, *J. Environ. Chem. Eng.*, 2021, **9**, 105259.

75 H. Li, X. Chen, D. Shen, F. Wu, R. Pleixats and J. Pan, *Nanoscale*, 2021, **13**, 15998–16016.

76 J. A. Melero, R. Van Grieken and G. Morales, *Chem. Rev.*, 2006, **106**, 3790–3812.

77 E. Doustkhah, J. Lin, S. Rostamnia, C. Len, R. Luque, X. Luo, Y. Bando, K. C. W. Wu, J. Kim, Y. Yamauchi and Y. Ide, *Chem.–Eur. J.*, 2019, **25**, 1614–1635.

78 G. Ziarani, S. Roshankar, F. Mohajer and A. Badiei, *Curr. Org. Chem.*, 2021, **25**, 361–387.

79 G. M. Ziarani, N. Lashgari and A. Badiei, *J. Mol. Catal. A: Chem.*, 2015, **397**, 166–191.

80 D. Margolese, J. A. Melero, S. C. Christiansen, B. F. Chmelka and G. D. Stucky, *Chem. Mater.*, 2000, **12**, 2448–2459.

81 B. Karimi and D. Zareyee, *J. Mater. Chem.*, 2009, **19**, 8665–8670.

82 M. Gómez-Cazalilla, J. M. Mérida-Robles, A. Gurbani, E. Rodríguez-Castellón and A. Jiménez-López, *J. Solid State Chem.*, 2007, **180**, 1130–1140.

83 A. Vinu, G. S. Kumar, K. Ariga and V. Murugesan, *J. Mol. Catal. A: Chem.*, 2005, **235**, 57–66.

84 M. K. Kolli, S. R. Dadireddy, P. Elamathi, G. Chandrasekar and S. Chidara, *Iran. J. Energy Environ.*, 2017, **8**, 305–317.

85 P. Zhang, H. Wu, M. Fan, W. Sun, P. Jiang and Y. Dong, *Fuel*, 2019, **235**, 426–432.

86 Ç. Yildirim, Ç. Yolaçan and F. Aydoğan, *Turk. J. Chem.*, 2012, **36**, 101–109.

87 J. S. Yadav, B. V. S. Reddy, B. Eeshwaraiah and M. Srinivas, *Tetrahedron*, 2004, **60**, 1767–1771.

88 M. Abid, M. Savolainen, S. Landge, J. Hu, G. K. S. Prakash, G. A. Olah and B. Török, *J. Fluorine Chem.*, 2007, **128**, 587–594.

89 Q. Wang, L. Peng, G. Li, P. Zhang, D. Li, F. Huang and Q. Wei, *Int. J. Mol. Sci.*, 2013, **14**, 12520–12532.

90 J. Wang, Y. Masui, K. Watanabe and M. Onaka, *Adv. Synth. Catal.*, 2009, **351**, 553–557.

91 J. Wang, Y. Masui and M. Onaka, *Eur. J. Org. Chem.*, 2010, 1763–1771.

92 Y. Masui, J. Wang, K. Teramura, T. Kogure, T. Tanaka and M. Onaka, *Microporous Mesoporous Mater.*, 2014, **198**, 129–138.

93 A. S. Amarasekara, *Chem. Rev.*, 2016, **116**, 6133–6183.

94 M. Sefat, D. Saberi and K. Niknam, *Catal. Lett.*, 2011, **141**, 1713–1720.

95 A. R. Moosavi-Zare, M. A. Zolfigol, M. Zarei, A. Zare and J. Afsar, *Appl. Catal., A*, 2015, **505**, 224–234.

96 G. Ziarani, L. Seiedakbari, P. Gholamzadeh and A. Badiei, *Iran. J. Catal.*, 2017, **7**, 137–145.

97 S. Wang, Q. Zhang, C. Cui, H. Niu, C. Wu and J. Wang, *Green Energy Environ.*, 2021, DOI: 10.1016/j.gee.2021.02.010.

98 F. Shirini, M. Seddighi, M. Mazloumi, M. Makhsous and M. Abedini, *J. Mol. Liq.*, 2015, **208**, 291–297.

99 P. Sutra and D. Brunel, *Chem. Commun.*, 1996, 2485–2486.

100 I. Chisem, J. Rafelt, J. Chisem, J. Clark, D. Macquarrie, M. Shieh, R. Jachuck, C. Ramshaw and K. Scott, *Chem. Commun.*, 1998, 1949–1950.

101 D. E. De Vos, M. Dams, B. F. Sels and P. A. Jacobs, *Chem. Rev.*, 2002, **102**, 3615–3640.

102 C. Baleizão and H. Garcia, *Chem. Rev.*, 2006, **106**, 3987–4043.

103 F. Rajabi, S. Ghiassian and M. R. Saidi, *Green Chem.*, 2010, **12**, 1349–1352.

104 F. Rajabi, S. Nourian, S. Ghiassian, A. M. Balu, M. R. Saidi, J. C. Serrano-Ruiz and R. Luque, *Green Chem.*, 2011, **13**, 3282–3289.

105 F. Rajabi, R. Luque, J. H. Clark, B. Karimi and D. J. Macquarrie, *Catal. Commun.*, 2011, **12**, 510–513.

106 B. Sun, G. Zhou and H. Zhang, *Prog. Solid State Chem.*, 2016, **44**, 1–19.

107 M. Jiang, S. Li, X. Shi, T. Gao, Z. Liu and G. Zhou, *RSC Adv.*, 2016, **6**, 76824–76828.

108 L. Wu, H. Zhang, M. Wu, Y. Zhong, X. Liu and Z. Jiao, *Microporous Mesoporous Mater.*, 2016, **228**, 318–328.

109 W. Zhang, M. Jiang, T. Gao, X. Sun and G. Zhou, *Colloids Surf., A*, 2018, **558**, 138–143.

110 D. Wang, X. Li, Z. Liu, X. Shi and G. Zhou, *Solid State Sci.*, 2017, **63**, 62–69.

111 J. Pang, G. Zhou, R. Liu and T. Li, *Mater. Sci. Eng., C*, 2016, **59**, 35–42.

112 M. B. Gawande, A. Goswami, T. Asefa, H. Guo, A. V. Biradar, D. L. Peng, R. Zboril and R. S. Varma, *Chem. Soc. Rev.*, 2015, **44**, 7540–7590.

113 M. Bodaghifard, M. Hamidinasab and N. Ahadi, *Curr. Org. Chem.*, 2018, **22**, 234–267.

114 S. Liu, B. Yu, S. Wang, Y. Shen and H. Cong, *Adv. Colloid Interface Sci.*, 2020, **281**, 102165.

115 L. M. Rossi, N. J. S. Costa, F. P. Silva and R. Wojcieszak, *Green Chem.*, 2014, **16**, 2906–2933.

116 H. L. Ding, Y. X. Zhang, S. Wang, J. M. Xu, S. C. Xu and G. H. Li, *Chem. Mater.*, 2012, **24**, 4572–4580.

117 N. Zhu, H. Ji, P. Yu, J. Niu, M. U. Farooq, M. W. Akram, I. O. Udego, H. Li and X. Niu, *Nanomaterials*, 2018, **8**, 810.

118 A. G. Niculescu, C. Chircov and A. M. Grumezescu, *Methods*, 2022, **199**, 16–27.

119 W. Stöber, A. Fink and E. Bohn, *J. Colloid Interface Sci.*, 1968, **26**, 62–69.

120 M. Ohmori and E. Matijević, *J. Colloid Interface Sci.*, 1992, **150**, 594–598.

121 L. Zhang, H. Shao, H. Zheng, T. Lin and Z. Guo, *Int. J. Miner., Metall. Mater.*, 2016, **23**, 1112–1118.

122 A. Habibi, E. Ghanbari and I. Yavari, *Arkivoc*, 2019, **vi**, 128–140.

123 F. K. Esfahani, D. Zareyee and R. Yousefi, *ChemCatChem*, 2014, **6**, 3333–3337.

124 A. Mobaraki, B. Movassagh and B. Karimi, *Appl. Catal., A*, 2014, **472**, 123–133.

125 D. Elhamifar, Z. Ramazani, M. Norouzi and R. Mirbagheri, *J. Colloid Interface Sci.*, 2018, **511**, 392–401.

126 A. Mobaraki, B. Movassagh and B. Karimi, *ACS Comb. Sci.*, 2014, **16**, 352–358.

127 B. Zhang, Y. Wang, J. Zhang, S. Qiao, Z. Fan, J. Wan and K. Chen, *Colloids Surf., A*, 2020, **586**, 124288.

128 M. Z. Kassaee, H. Masrouri and F. Movahedi, *Appl. Catal., A*, 2011, **395**, 28–33.

129 M. Yarie, M. Zolfigol, Y. Bayat, A. Asgari, D. Alonso and A. Khoshnood, *RSC Adv.*, 2016, **6**, 82842–82853.

130 Q. Zhang, H. Su, J. Luo and Y. Wei, *Green Chem.*, 2012, **14**, 201–208.

131 A. Maleki, S. Azadegan and J. Rahimi, *Appl. Organomet. Chem.*, 2019, **33**, e4810.

132 G. Fang, H. Chen, Y. Zhang and A. Chen, *Int. J. Biol. Macromol.*, 2016, **88**, 189–195.

133 F. Karimi, M. Yarie and M. A. Zolfigol, *Mol. Catal.*, 2020, **489**, 110924.

134 H. Fatahi, M. Jafarzadeh and Z. Pourmanouchehri, *J. Heterocycl. Chem.*, 2019, **56**, 2090–2098.

135 M. Jafarzadeh, E. Soleimani, P. Norouzi, R. Adnan and H. Sepahvand, *J. Fluorine Chem.*, 2015, **178**, 219–224.

136 A. Mokkarat, S. Kruanetr and U. Sakee, *J. Mol. Struct.*, 2022, **1259**, 132745.

137 M. Köckinger, C. A. Hone and C. O. Kappe, *Org. Lett.*, 2019, **21**, 5326–5330.

138 M. Takamura, Y. Hamashima, H. Usuda, M. Kanai and M. Shibasaki, *Angew. Chem., Int. Ed.*, 2000, **39**, 1650–1652.

139 M. Kazemnejadi, S. A. Alavi G, Z. Rezazadeh, M. A. Nasseri, A. Allahresani and M. Esmaeilpour, *Appl. Organomet. Chem.*, 2019, **34**, e5388.

140 M. Sun, W. Liu, W. Wu, Q. Li, D. Song, L. Yan and M. Mohammadnia, *Inorg. Nano-Met. Chem.*, 2021, DOI: 10.1080/24701556.2021.1977819.

141 J. Rakhtshah, B. Shaabani, S. Salehzadeh and N. Hosseinpour Moghadam, *Bioorg. Chem.*, 2019, **85**, 420–430.

142 K. Ruiz-Mirazo, C. Briones and A. De la Escosura, *Chem. Rev.*, 2013, **114**, 285–366.

143 J. D. Sutherland, *Angew. Chem., Int. Ed.*, 2015, **55**, 104–121.

144 S. K. Singh, C. Zhu, J. La Jeunesse, R. C. Fortenberry and R. I. Kaiser, *Nat. Commun.*, 2022, **13**, 375.

145 C. S. Foden, S. Islam, C. Fernández-García, L. Maugeri, T. D. Sheppard and M. W. Powner, *Science*, 2020, **370**, 865–869.

146 J. Singh, D. Whitaker, B. Thoma, S. Islam, C. S. Foden, A. E. Aliev, T. D. Sheppard and M. W. Powner, *J. Am. Chem. Soc.*, 2022, **144**, 10151–10155.

147 T. Stolar, S. Grubešić, N. Cindro, E. Meštrović, K. Užarević and J. G. Hernández, *Angew. Chem., Int. Ed.*, 2021, **60**, 12727–12731.

148 H. Bu, P. Yuan, H. Liu, D. Liu, Z. Qin, X. Zhong, H. Song and Y. Li, *Chem. Geol.*, 2019, **510**, 72–83.

149 M. Faustini, L. Nicole, E. Ruiz-Hitzky and C. Sanchez, *Adv. Funct. Mater.*, 2018, **28**, 1704158.

150 C. Lee, J. M. Weber, L. E. Rodriguez, R. Y. Sheppard, L. M. Barge, E. L. Berger and A. S. Burton, *Symmetry*, 2022, **14**, 460.

151 Q. Sallembien, L. Bouteiller, J. Crassous and M. Raynal, *Chem. Soc. Rev.*, 2022, **51**, 3436–3476.

152 C. Nájera and J. M. Sansano, *Chem. Rev.*, 2007, **107**, 4584–4671.

153 J. Wang, X. Liu and X. Feng, *Chem. Rev.*, 2011, **111**, 6947–6983.

154 S. Miyagawa, K. Yoshimura, Y. Yamazaki, N. Takamatsu, T. Kuraish, S. Aiba, Y. Tokunaga and T. Kawasaki, *Angew. Chem., Int. Ed.*, 2016, **56**, 1055–1058.

155 X. H. Cai and B. Xie, *Arkivoc*, 2014, **i**, 205–248.

156 N. Kurono and T. Ohkuma, *ACS Catal.*, 2016, **6**, 989–1023.

157 U. Díaz and A. Corma, *Chem.–Eur. J.*, 2018, **24**, 3944–3958.

158 G. Szőllősi, *Catal. Sci. Technol.*, 2018, **8**, 389–422.

159 C. Simons, U. Hanefeld, I. W. C. E. Arends, A. J. Minnaard, T. Maschmeyer and R. A. Sheldon, *Chem. Commun.*, 2004, 2830–2831.

160 D. Feng, J. Xu, J. Wan, B. Xie and X. Ma, *Catal. Sci. Technol.*, 2015, **5**, 2141–2148.

161 J. Safaei-Ghomi and S. Zahedi, *Tetrahedron Lett.*, 2016, **57**, 1071–1073.

162 P. García-García, A. Zagdoun, C. Copéret, A. Lesage, U. Díaz and A. Corma, *Chem. Sci.*, 2013, **4**, 2006–2012.

163 J. Safaei-Ghomi and S. Zahedi, *Appl. Organomet. Chem.*, 2015, **29**, 566–571.

164 S. Chongdar, S. Bhattacharjee, P. Bhanja and A. Bhaumik, *Chem. Commun.*, 2022, **58**, 3429–3460.

165 A. M. Nauth and T. Opatz, *Org. Biomol. Chem.*, 2019, **17**, 11–23.

166 C. Grundke and T. Opatz, *Green Chem.*, 2019, **21**, 2362–2366.

167 C. Bolm, R. Mocci, C. Schumacher, M. Turberg, F. Puccetti and J. G. Hernández, *Angew. Chem., Int. Ed.*, 2018, **57**, 2423–2426.

168 T. Keijer, V. Bakker and J. C. Slootweg, *Nat. Chem.*, 2019, **11**, 190–195.

169 S. V. Mohan and R. Katakojwala, *Curr. Opin. Green Sustainable Chem.*, 2021, **28**, 100434.